Mixed Quantum-Classical Methods based on Exact Factorization

Daeho Han

Department of Chemistry,
University at Buffalo, SUNY

July 10, 2024

Outline

- Conventional mixed quantum-classical (MQC) methods
- The exact factorization (XF) formalism & its MQC variation
- Coupled-trajectory (CT) MQC approach
- Independent-trajectory XF methods
- Implementation of the XF methods in Libra

Conventional mixed quantum-classical (MQC) methods

Effective potential energy surfaces in the MQC methods

- In the mixed quantum-classical methods, nuclear and electronic degrees of freedom (DOF) are described separately: electrons are treated as quantum particles, and nuclei are approximated to classical particles.

- The simplest form of the MQC approach is the Born-Oppenheimer molecular dynamics (BOMD) – molecular dynamics on the single potential energy surface (PES).

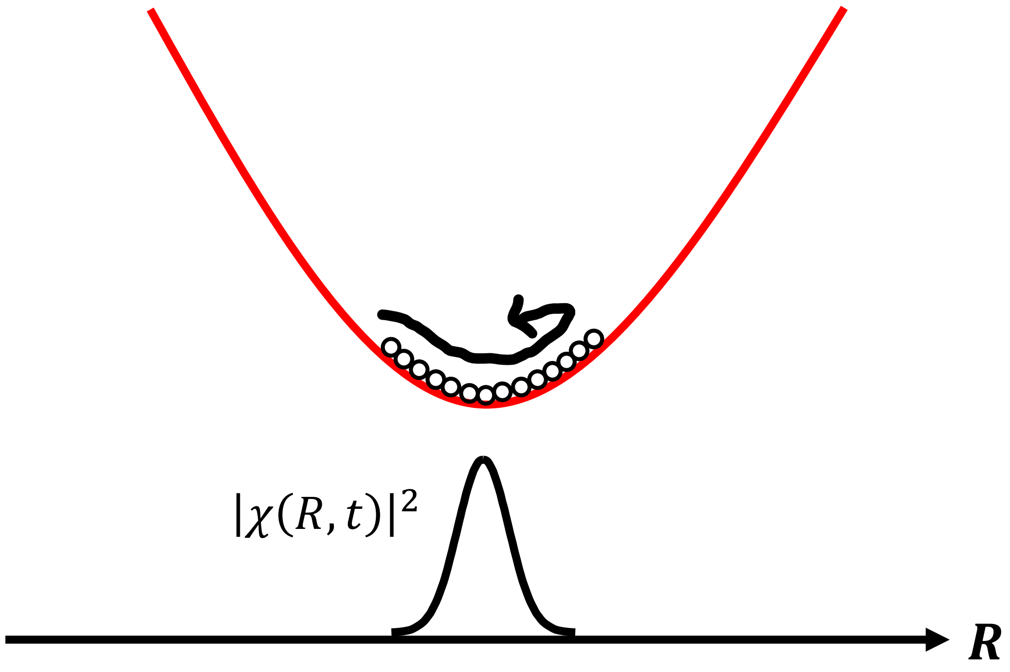

The classical ensemble of the particle reflects on the quantum nuclear distribution.

$$\Psi(\boldsymbol{r},\boldsymbol{R},t) \approx \chi_i(\boldsymbol{R},t)\Phi_i(\boldsymbol{r};\boldsymbol{R}(t))$$

$$\begin{cases} M_\nu \ddot{R}_\nu(t) = -\nabla_\nu E_i(\boldsymbol{R}) \\ H_{BO}\Phi_i(\boldsymbol{r};\boldsymbol{R}(t)) = E_i(\boldsymbol{R})\Phi_i(\boldsymbol{r};\boldsymbol{R}(t)) \end{cases}$$

Effective potential energy surfaces in the MQC methods

- Then how do we set the proper potential energies in the nonadiabatic regime?

Surface hopping

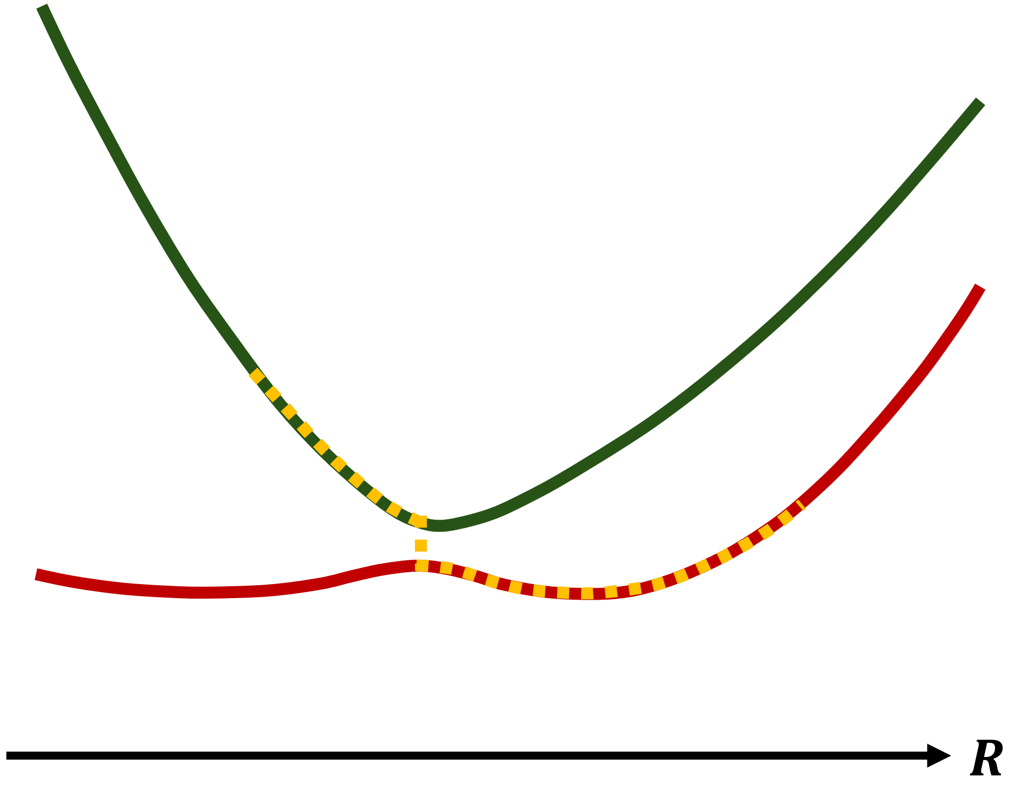

Stochastically determined adiabatic force

↔ intuitively correct but discontinuous PES

Ehrenfest

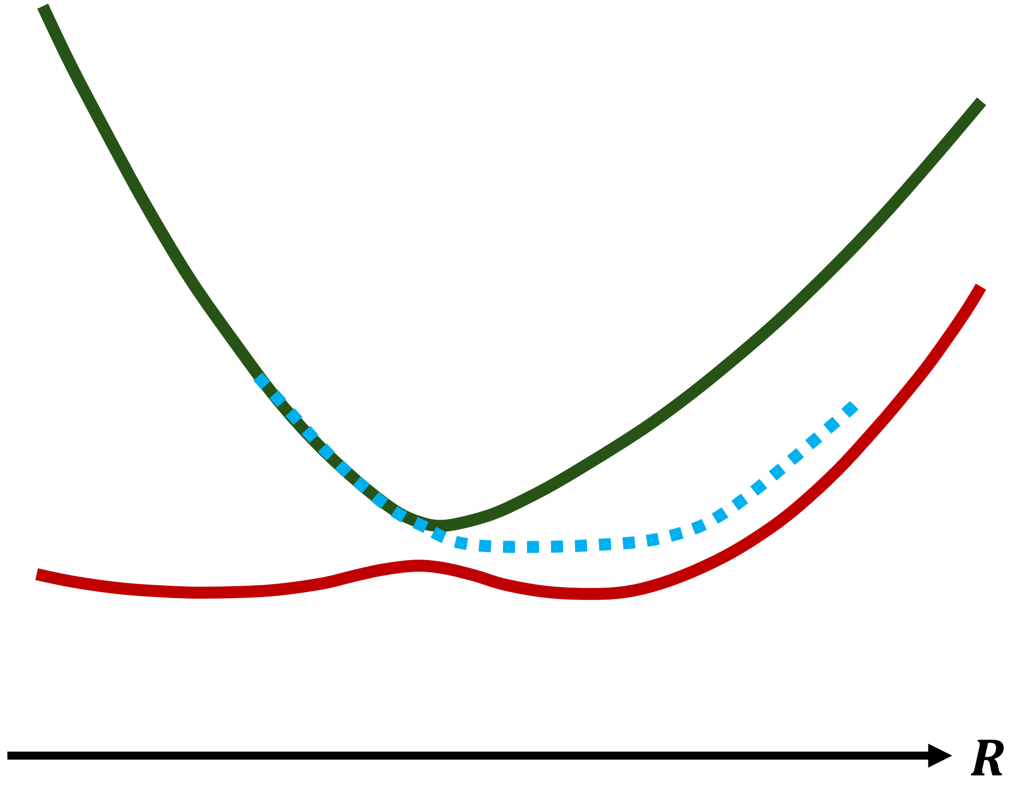

Mean-field force

↔ unphysical pathway and wrong branching ratio

Decoherence correction in the MQC methods

- "Overcoherence" problem: the decoherence is missing in the original electronic TDSE.

$$\dot{C}_i = -\frac{i}{\hbar}E_i C_i - \sum_j C_j \sum_\nu \dot{R}_\nu \cdot d_{ij,\nu}$$

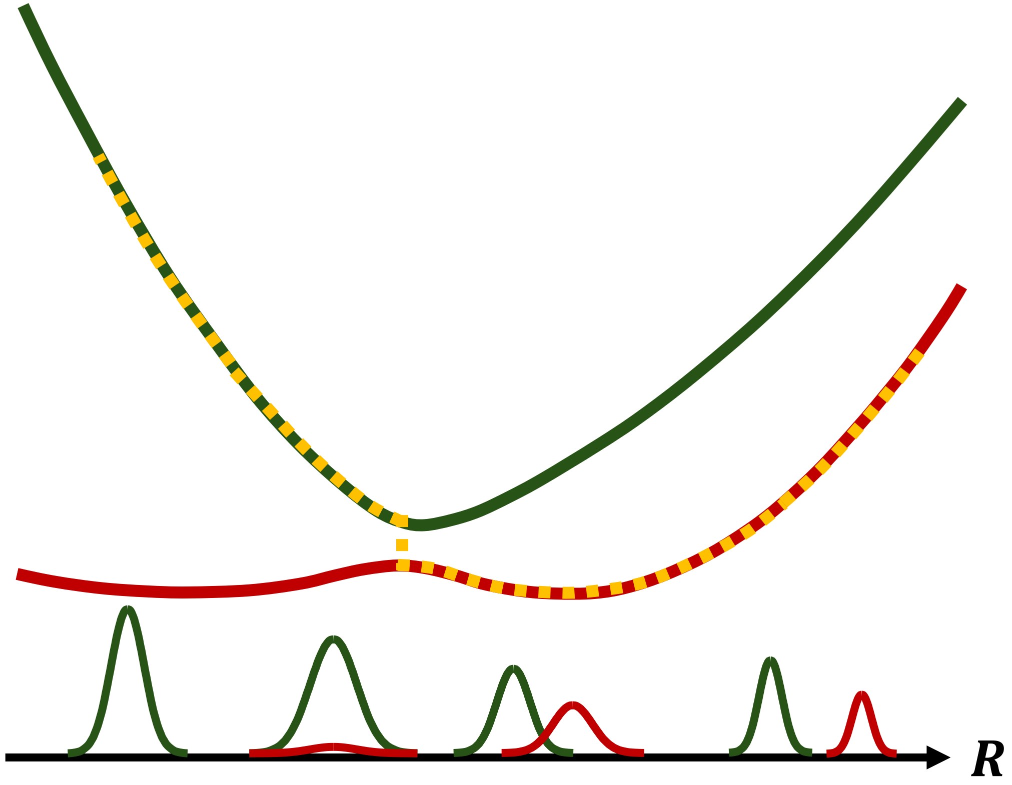

The population exchange only occurs when the nonadiabatic coupling (NAC) is finite.

The first term only change the phase of the adiabatic coefficient.

Without the decoherence correction, there could be long-lasting coherence.

Decoherence correction in the MQC methods

- “Overcoherence” problem: the decoherence is missing in the original electronic TDSE.

$$\dot{C}_i = -\frac{i}{\hbar} E_i C_i - \sum_j C_j \sum_\nu \dot{R}_\nu \cdot d_{ij,\nu}$$

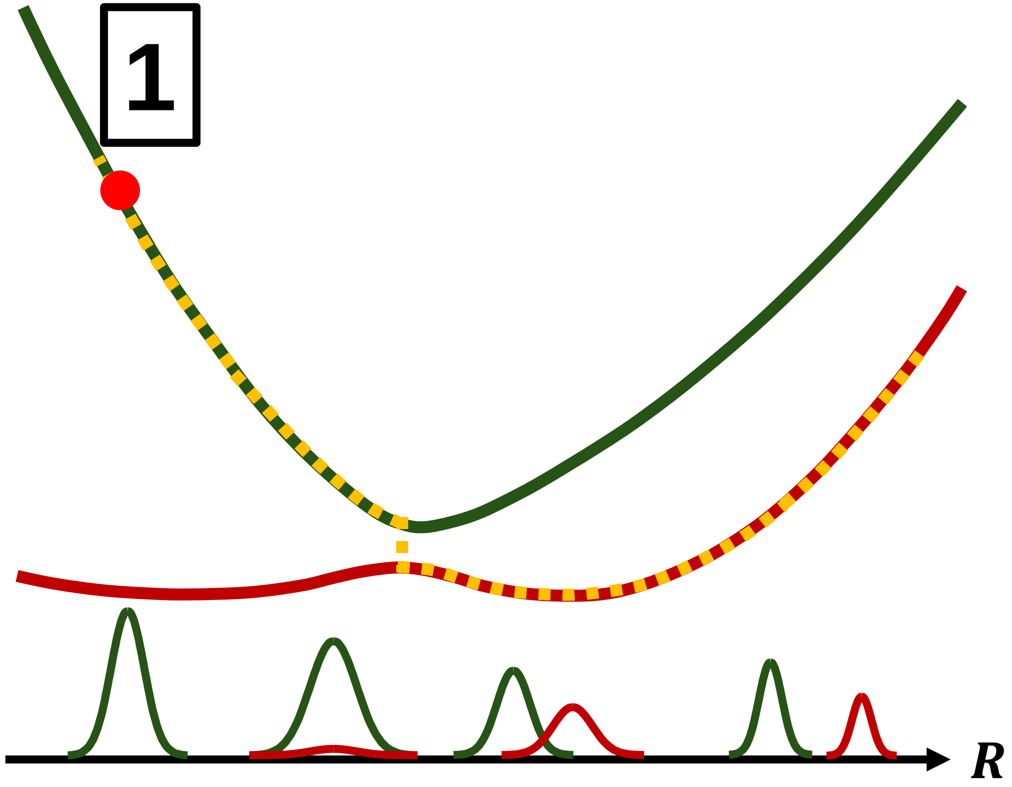

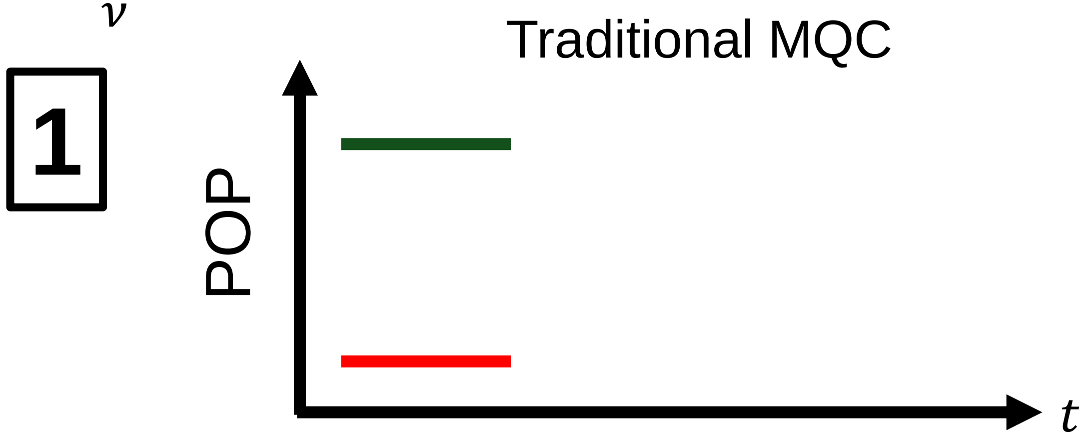

$$P_i = |C_i|^2$$

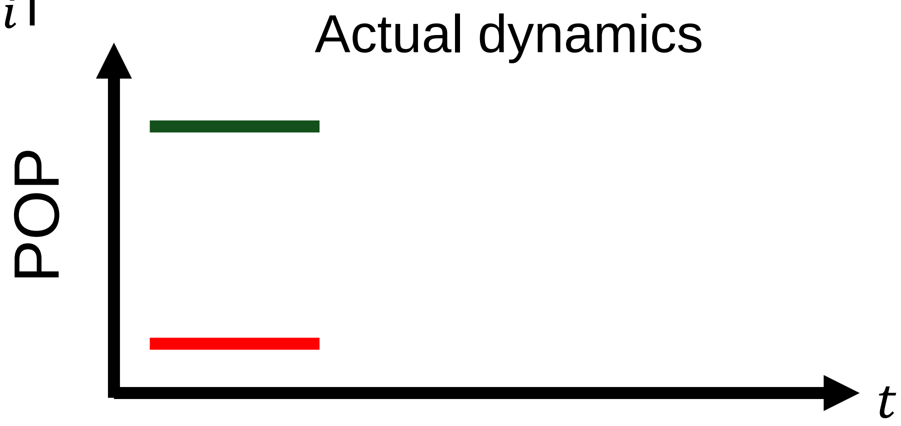

Decoherence correction in the MQC methods

- "Overcoherence" problem: the decoherence is missing in the original electronic TDSE.

$$\dot{C}_i = -\frac{i}{\hbar}E_i C_i - \sum_j C_j \sum_\nu \dot{R}_\nu \cdot d_{ij,\nu}$$

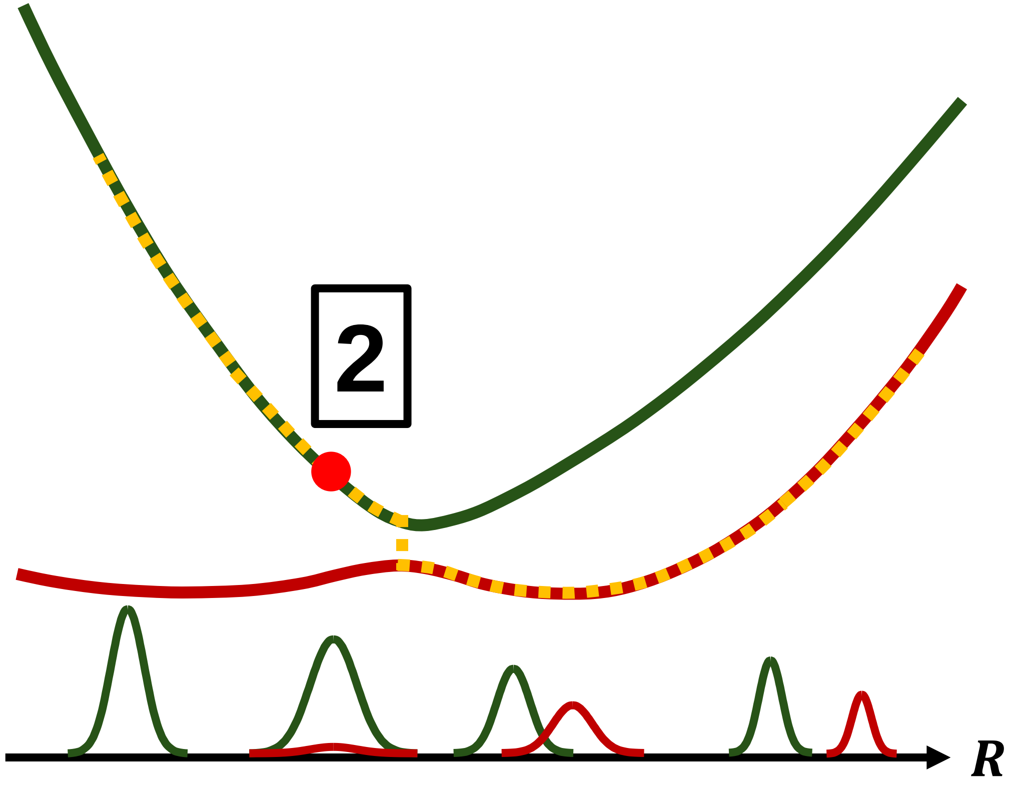

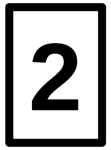

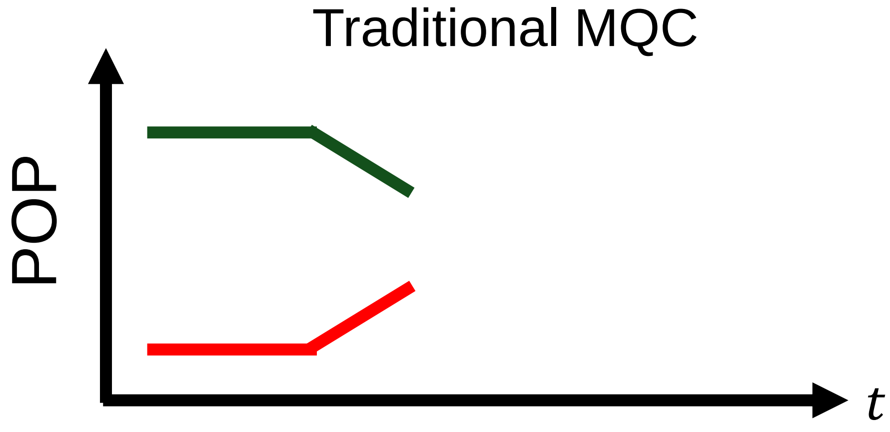

$$P_i = |C_i|^2$$

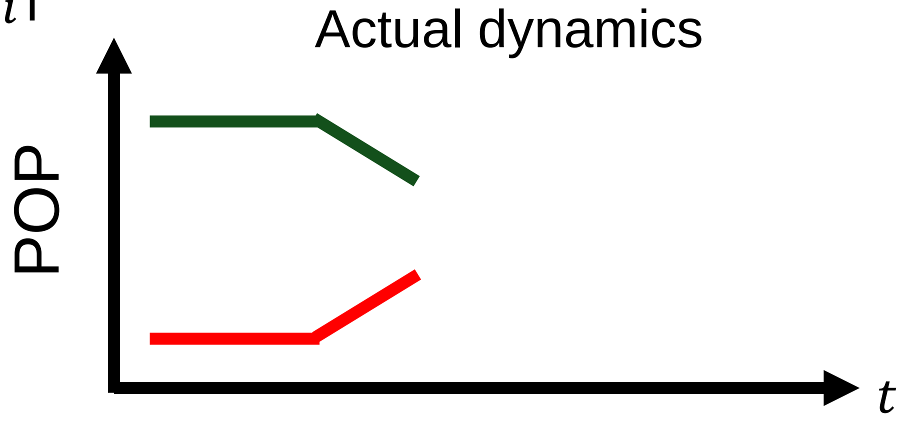

Decoherence correction in the MQC methods

- "Overcoherence" problem: the decoherence is missing in the original electronic TDSE.

$$\dot{C}_i = -\frac{i}{\hbar} E_i C_i - \sum_j C_j \sum_\nu \dot{R}_\nu \cdot d_{ij,\nu}$$

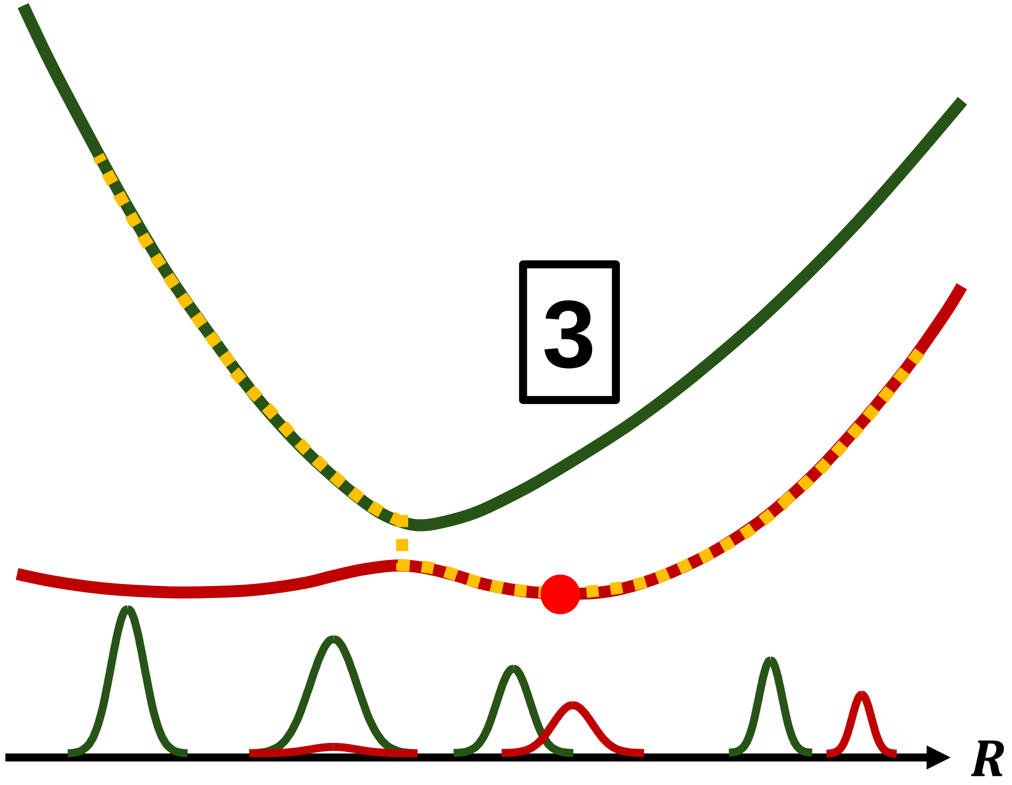

Traditional MQC

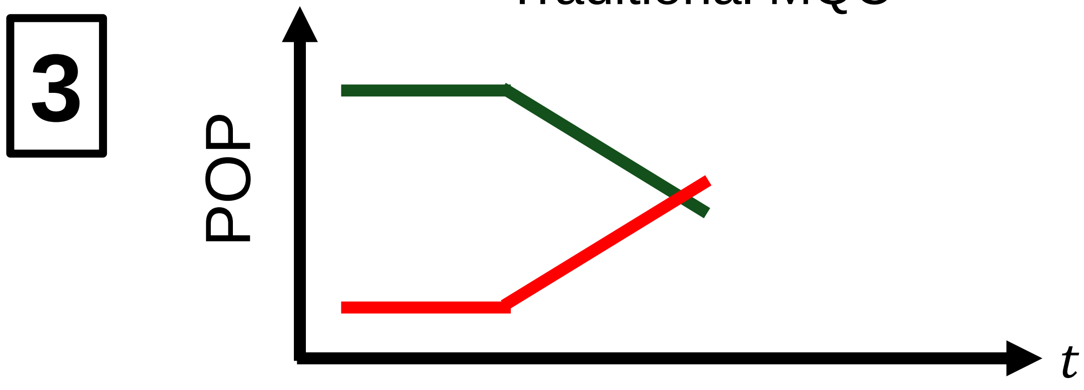

$$P_i = |C_i|^2$$

Actual dynamics

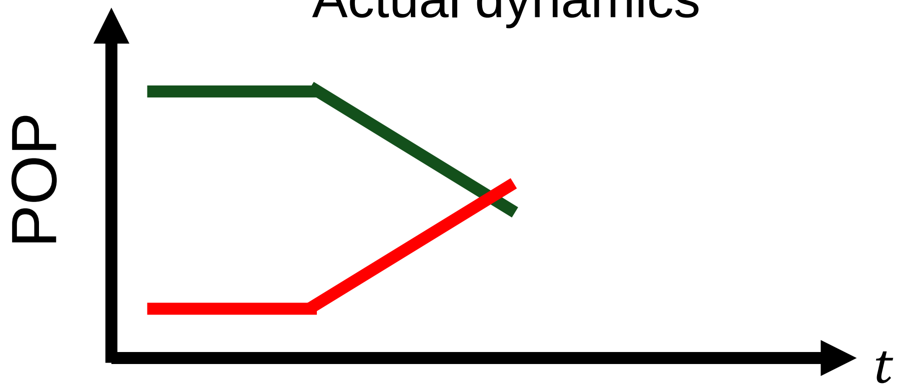

Decoherence correction in the MQC methods

- "Overcoherence" problem: the decoherence is missing in the original electronic TDSE.

$$\dot{C}_i = -\frac{i}{\hbar}E_i C_i - \sum_j C_j \sum_\nu \dot{R}_\nu \cdot d_{ij,\nu}$$

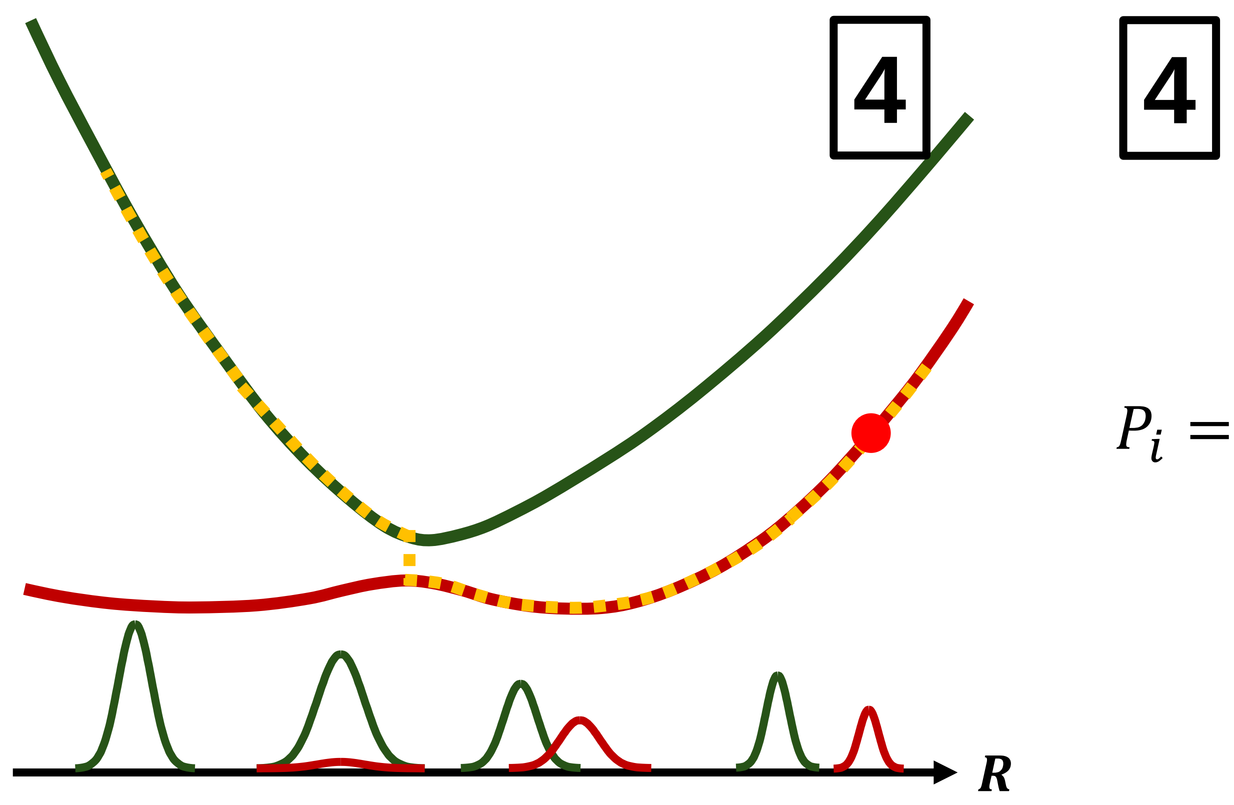

$$P_i = |C_i|^2$$

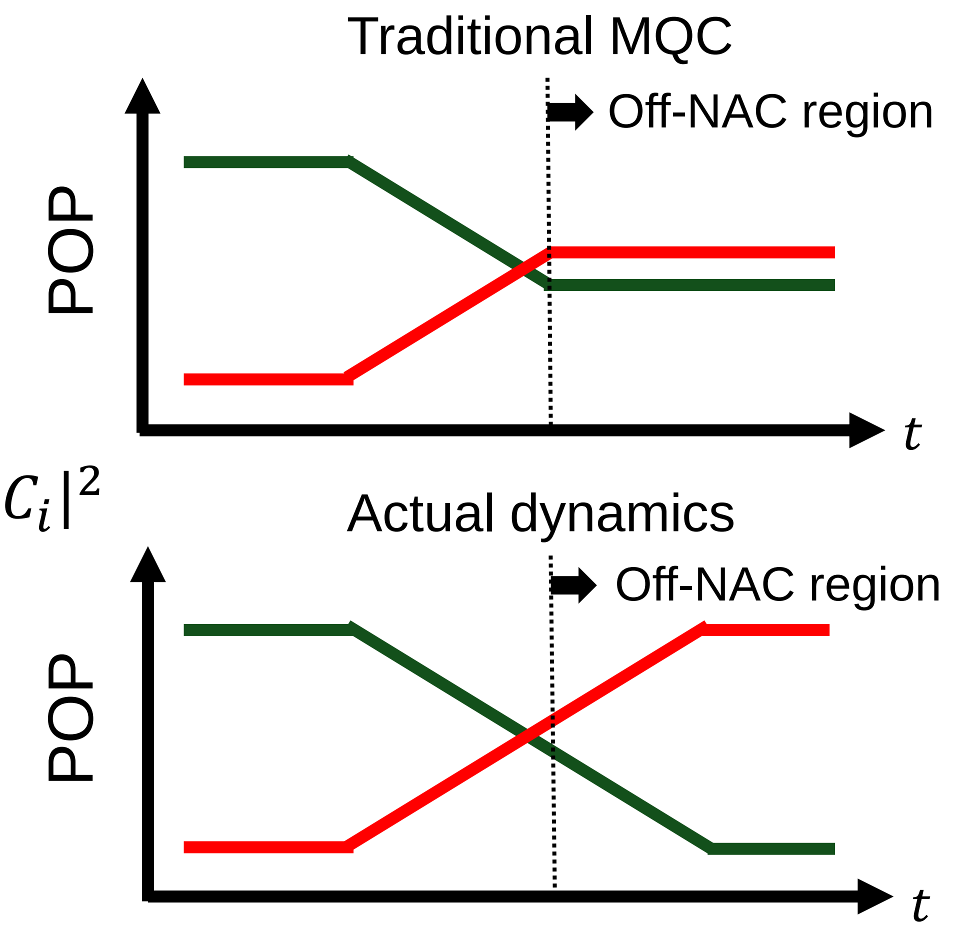

Effective potential energy surfaces in the MQC methods

- To resolve this overcoherence problem, various decoherence-corrected methods have been developed. The decoherence correction has various types, which correct the electronic TDSE directly or decoherence times.

Simplified Decay of Mixing (SDM)

Granucci, G.; Persico, M. *JCP.* **2007**, *126* (13), 134114.

$$\tau_{ia} = -\frac{\hbar}{|E_i - E_a|}\left(1 + \frac{C}{E_{kin}}\right)C_i \qquad C_{i\neq a} := C_{i\neq a}\exp\left(-\frac{\Delta t}{t_{ia}}\right)$$

A-FSSH

Jain, A.; Alguire, E.; Subotnik, J. E. *JCTC.* **2016**, *12* (11), 5256–5268.

$$\tau_{ij}^{-1} = \frac{\delta\boldsymbol{F}_{ii}\cdot(\delta\boldsymbol{R}_{ii} - \delta\boldsymbol{R}_{jj})}{2\hbar} - \frac{2\left|\boldsymbol{d}_{ji}\cdot(E_j - E_i)(\delta\boldsymbol{R}_{ii} - \delta\boldsymbol{R}_{jj})\cdot\boldsymbol{v}\right|}{\hbar\boldsymbol{v}\cdot\boldsymbol{v}}$$

Instantaneous Decoherence Approximation (IDA)

Nelson, T.; Fernandez-Alberti, S.; Roitberg, A. E.; Tretiak, S. *JCP.* **2013**, *138* (22), 224111.

Mean-field dynamics with stochastic decoherence (MFSD)

Bedard-Hearn, M. J.; Larsen, R. E.; Schwartz, B. J. *JCP.* **2005**, *123* (23), 234106.

$$\tau_i^{-2} = \sum_{\nu}\frac{\left(\boldsymbol{F}_{\nu}(0) - \boldsymbol{F}_{i,\nu}\right)^2}{4a_{\nu}\hbar^2}$$

Decoherence-Induced Surface Hopping (DISH)

Jaeger, H. M.; Fischer, S.; Prezhdo, O. V. *JCP.* **2012**, *137* (22), 22A545.

$$\tau_i^{-1} = \sum_{j\neq i}\left|C_j\right|^2 r_{ij}$$

The exact factorization (XF) formalism
&
its MQC variation

XF ansatz

- Molecular wave function is factored into the nuclear and electronic wave functions (WFCs).

$$\Psi(\boldsymbol{r},\boldsymbol{R},t) = \chi(\boldsymbol{R},t)\Phi_{\boldsymbol{R}}(\boldsymbol{r},t)$$

$$\forall \boldsymbol{R} \int |\Phi_{\boldsymbol{R}}(\boldsymbol{r},t)|^2 \, d\boldsymbol{r} = 1$$ Partial Normalization Condition

$$\Rightarrow \quad |\Psi(\boldsymbol{r},\boldsymbol{R},t)|^2 d\boldsymbol{r}d\boldsymbol{R} = |\chi(\boldsymbol{R},t)|^2 d\boldsymbol{R} \times |\Phi_{\boldsymbol{R}}(\boldsymbol{r},t)|^2 d\boldsymbol{r}$$

Total probability — Marginal probability for $\boldsymbol{R}$ — Conditional probability for $\boldsymbol{r}$ under $\boldsymbol{R}$

- The probability amplitude $|\chi|^2$ stands for the exact time-dependent nuclear density.

$$|\chi(\boldsymbol{R},t)|^2 = \sum_i^{\infty} |\chi_i(\boldsymbol{R},t)|^2$$

cf. Born-Huang expansion

$$\Psi(\boldsymbol{r},\boldsymbol{R},t) = \sum_i^{\infty} \chi_i(\boldsymbol{R},t)\Phi_i(\boldsymbol{r};\boldsymbol{R}(t))$$

Abedi, A.; Maitra, N. T.; Gross, E. K. U. *PRL* **2010**, *105* (12), 123002.

Abedi, A.; Maitra, N. T.; Gross, E. K. U. *JCP* **2012**, *137* (22), 22A530.

XF ansatz

- Coupled XF equations

$$\begin{cases} i\hbar\partial_t\chi(\boldsymbol{R},t) = \left(\sum_\nu \frac{[-i\hbar\nabla_\nu + A_\nu(\boldsymbol{R},t)]^2}{2M_\nu} + \epsilon(\boldsymbol{R},t)\right)\chi(\boldsymbol{R},t) \\ i\hbar\partial_t\Phi_{\boldsymbol{R}}(\boldsymbol{r},t) = \left(H_{BO}(r,\boldsymbol{R}) + U_{en}^{coup}[\Phi_{\boldsymbol{R}},\chi] - \epsilon(\boldsymbol{R},t)\right)\Phi_{\boldsymbol{R}}(\boldsymbol{R},t) \end{cases}$$

<u>Time-dependent (TD) PES</u>

$$\epsilon(\boldsymbol{R},t) = \left\langle \Phi_{\boldsymbol{R}}(t) \middle| H_{BO} + U_{en}^{coup} - i\hbar\partial_t \middle| \Phi_{\boldsymbol{R}}(t) \right\rangle_{\boldsymbol{r}}$$

<u>TD vector potential</u>

$$A_\nu(\boldsymbol{R},t) = \langle \Phi_{\boldsymbol{R}}(t) | -i\hbar\nabla_\nu \Phi_{\boldsymbol{R}}(t) \rangle_{\boldsymbol{r}}$$

<u>Electron-nuclear correlation operator</u>

$$U_{en}^{coup}[\Phi_{\boldsymbol{R}},\chi] = \sum_\nu \frac{1}{M_\nu}\left[\frac{[-i\hbar\nabla_\nu - A_\nu(\boldsymbol{R},t)]^2}{2} + \left(\frac{-i\hbar\nabla_\nu\chi}{\chi} + A_\nu(\boldsymbol{R},t)\right)\cdot\left(-i\hbar\nabla_\nu - A_\nu(\boldsymbol{R},t)\right)\right]$$

Leading to Diagonal BO correction | Major electron-nuclear correlation

Abedi, A.; Maitra, N. T.; Gross, E. K. U. *PRL.* **2010**, *105* (12), 123002.
Abedi, A.; Maitra, N. T.; Gross, E. K. U. *JCP.* **2012**, *137* (22), 22A530.

Towards the MQC equations

- Inserting the polar form of nuclear WFC, $\chi(R,t) = |\chi(\boldsymbol{R},t)| \exp\left(\frac{i}{\hbar} S(\boldsymbol{R},t)\right)$, into the nuclear TDSE:

Real part

$$\partial_t S(\boldsymbol{R},t) = -\sum_\nu \frac{[\nabla_\nu S(\boldsymbol{R},t) + A_\nu(\boldsymbol{R},t)]^2}{2M_\nu} - \epsilon(\boldsymbol{R},t) + \hbar^2 \sum_\nu \frac{1}{2M_\nu} \frac{\nabla_\nu^2 |\chi(\boldsymbol{R},t)|}{|\chi(\boldsymbol{R},t)|}$$

Quantum Hamilton-Jacobi equation

Imaginary part

$$\partial_t |\chi(\boldsymbol{R},t)|^2 = \sum_\nu -\frac{1}{M_\nu} \nabla_\nu \cdot \left[\left(\nabla_\nu S(\boldsymbol{R},t) + \boldsymbol{A}_\nu(\boldsymbol{R},t)\right)|\chi(\boldsymbol{R},t)|^2\right]$$

Continuity equation → Throw away
(Within MQC, we assume its solution, i.e., a delta function).

cf. Hamilton-Jacobi equation

$$\partial_t S + H(\boldsymbol{R}, \boldsymbol{\nabla}_{\boldsymbol{R}} S, t) = 0$$

Min, S. K.; Agostini, F.; Gross, E. K. U. *PRL.* **2015**, *115* (7), 073001.
Agostini, F.; Min, S. K.; Abedi, A.; Gross, E. K. U. *JCTC.* **2016**, *12* (5), 2127–2143.

Towards the MQC equations

- Identifying the classical momentum: $P_\nu = \nabla_\nu S + A_\nu$ by neglecting the quantum potential.

$$\partial_t S(\boldsymbol{R},t) \approx -\sum_\nu \frac{[\nabla_\nu S(\boldsymbol{R},t) + A_\nu(\boldsymbol{R},t)]^2}{2M_\nu} - \epsilon(\boldsymbol{R},t)$$

➡ $$\dot{S}(\boldsymbol{R},t) = -\sum_\nu \left[\frac{[\nabla_\nu S(\boldsymbol{R},t) + A_\nu(\boldsymbol{R},t)]^2}{2M_\nu} - \frac{P_\nu}{M_\nu}\cdot\nabla_\nu S(\boldsymbol{R},t)\right] - \epsilon(\boldsymbol{R},t)$$ In the Lagrangian frame

$$= -\sum_\nu \left[\frac{P_\nu^2}{2M_\nu} - \frac{P_\nu}{M_\nu}\cdot(P_\nu - A_\nu)\right] - \epsilon(\boldsymbol{R},t) = -\left(-\sum_\nu \frac{P_\nu^2}{2M_\nu} + \epsilon(\boldsymbol{R},t) + \sum_\nu A_\nu \cdot \frac{P_\nu}{M_\nu}\right)$$

Applying ∇_μ

➡ $\nabla_\mu\left(\frac{d}{dt}S\right) = \frac{d}{dt}(\nabla_\mu S) = \dot{P}_\mu - \dot{A}_\mu = -\nabla_\mu\left(\epsilon(\boldsymbol{R},t) + \sum_\nu A_\nu \cdot \frac{P_\nu}{M_\nu}\right) \coloneqq 0$ (by setting the Gauge condition)

$\therefore \dot{P}_\mu = \dot{A}_\mu$ under $\epsilon(\boldsymbol{R},t) + \sum_\nu A_\nu \cdot \frac{P_\nu}{M_\nu} = 0$

Min, S. K.; Agostini, F.; Gross, E. K. U. *PRL* **2015**, *115* (7), 073001.

Agostini, F.; Min, S. K.; Abedi, A.; Gross, E. K. U. *JCTC* **2016**, *12* (5), 2127–2143.

Towards the MQC equations

- Approximation to the electronic TDSE

$$i\hbar\partial_t\Phi_{\boldsymbol{R}}(\boldsymbol{r},t) = \big(H_{BO}(r,\boldsymbol{R}) + U_{en}^{coup}[\Phi_{\boldsymbol{R}},\chi] - \epsilon(\boldsymbol{R},t)\big)\chi(\boldsymbol{R},t)$$

Neglecting the 2nd order terms generating the DBOC contribution

$$U_{en}^{coup}[\Phi_{\boldsymbol{R}},\chi] \approx \sum_{\nu}\frac{1}{M_\nu}\left(\frac{-i\hbar\nabla_\nu\chi}{\chi} + A_\nu(\boldsymbol{R},t)\right)\cdot\left(-i\hbar\nabla_\nu - A_\nu(\boldsymbol{R},t)\right)$$

$$\Rightarrow \quad i\hbar\dot{\Phi}_{\boldsymbol{R}}(\boldsymbol{r},t) - i\hbar\sum_{\nu}\frac{P_\nu}{M_\nu}\cdot\nabla_\nu\Phi_{\boldsymbol{R}}(\boldsymbol{r},t)$$

$$= \left(H_{BO}(r,\boldsymbol{R}) + \sum_{\nu}\frac{1}{M_\nu}\left(\frac{-i\hbar\nabla_\nu\chi}{\chi} + A_\nu(\boldsymbol{R},t)\right)\cdot\left(-i\hbar\nabla_\nu - A_\nu(\boldsymbol{R},t)\right) - \epsilon(\boldsymbol{R},t)\right)\Phi_{\boldsymbol{R}}(\boldsymbol{r},t)$$

Min, S. K.; Agostini, F.; Gross, E. K. U. *PRL* **2015**, *115* (7), 073001.

Agostini, F.; Min, S. K.; Abedi, A.; Gross, E. K. U. *JCTC* **2016**, *12* (5), 2127–2143.

Towards the MQC equations

- Approximation to the electronic TDSE

$$i\hbar\dot{\Phi}_{\boldsymbol{R}}(\boldsymbol{r},t) = \left(H_{BO}(r,\boldsymbol{R}) + \sum_{\nu}\frac{1}{M_\nu}\left(\frac{-i\hbar\nabla_\nu\chi}{\chi} + A_\nu(\boldsymbol{R},t) - P_\nu\right)\cdot(-i\hbar\nabla_\nu)\right)\Phi_{\boldsymbol{R}}(\boldsymbol{r},t)$$

$$-\left[\sum_{\nu}\frac{1}{M_\nu}\left(\frac{-i\hbar\nabla_\nu\chi}{\chi} + A_\nu(\boldsymbol{R},t)\right)\cdot A_\nu(\boldsymbol{R},t) + \epsilon(\boldsymbol{R},t)\right]\Phi_{\boldsymbol{R}}(\boldsymbol{r},t)$$

Utilizing the polar form

$$\frac{-i\hbar\nabla_\nu\chi}{\chi} + A_\nu(\boldsymbol{R},t) = \nabla_\nu S + A_\nu(\boldsymbol{R},t) - i\hbar\frac{\nabla_\nu|\chi(\boldsymbol{R},t)|}{|\chi(\boldsymbol{R},t)|} = P_\nu + \mathcal{P}_\nu$$

Quantum momentum

$$\mathcal{P}_\nu = -i\hbar\frac{\nabla_\nu|\chi(\boldsymbol{R},t)|}{|\chi(\boldsymbol{R},t)|}$$

➡ $$i\hbar\dot{\Phi}_{\boldsymbol{R}}(\boldsymbol{r},t) = \left(H_{BO}(r,\boldsymbol{R}) + \sum_{\nu}\frac{\mathcal{P}_\nu}{M_\nu}\cdot(-i\hbar\nabla_\nu)\right)\Phi_{\boldsymbol{R}}(\boldsymbol{r},t)$$

$$-\left[\sum_{\nu}\frac{\mathcal{P}_\nu}{M_\nu}\cdot A_\nu(\boldsymbol{R},t) + \left(\sum_{\nu}\frac{P_\nu}{M_\nu}\cdot A_\nu(\boldsymbol{R},t) + \epsilon(\boldsymbol{R},t)\right)\right]\Phi_{\boldsymbol{R}}(\boldsymbol{r},t)$$

≡ 0 (The Gauge condition)

➡ $$i\hbar\dot{\Phi}_{\boldsymbol{R}}(\boldsymbol{r},t) = \left(H_{BO}(r,\boldsymbol{R}) - \sum_{\nu}\frac{\mathcal{P}_\nu}{M_\nu}\cdot\left(A_\nu(\boldsymbol{R},t) + i\hbar\nabla_\nu\right)\right)\Phi_{\boldsymbol{R}}(\boldsymbol{r},t)$$

Min, S. K.; Agostini, F.; Gross, E. K. U. *PRL* **2015**, *115* (7), 073001.

Agostini, F.; Min, S. K.; Abedi, A.; Gross, E. K. U. *JCTC* **2016**, *12* (5), 2127–2143.

Towards the MQC equations

- The XFMQC equations

$$i\hbar\dot{\Phi}_{\boldsymbol{R}}(\boldsymbol{r},t) = \left(H_{BO}(r,\boldsymbol{R}) - \sum_{\nu}\frac{\mathcal{P}_\nu}{M_\nu}\cdot\left(A_\nu(\boldsymbol{R},t) + i\hbar\nabla_\nu\right)\right)\Phi_{\boldsymbol{R}}(\boldsymbol{r},t)$$

$$\boldsymbol{F}_\nu = -\langle\Phi_{\boldsymbol{R}}(t)|\nabla_\nu H_{BO}|\Phi_{\boldsymbol{R}}(t)\rangle_{\boldsymbol{r}} + \sum_{\mu}\frac{2i\mathcal{P}_\mu}{\hbar M_\mu}\cdot\left(A_\mu(\boldsymbol{R},t)A_\nu(\boldsymbol{R},t) - \hbar^2\left\langle\nabla_\mu\Phi_{\boldsymbol{R}}(t)\middle|\nabla_\nu\Phi_{\boldsymbol{R}}(t)\right\rangle_{\boldsymbol{r}}\right)$$

Beyond the conventional Ehrenfest terms, the resulting coupled TDSEs explicitly contain the electron-nuclear correlation terms arising from the XF formalism, without adding any ad hoc decoherence correction.

Min, S. K.; Agostini, F.; Gross, E. K. U. *PRL* **2015**, *115* (7), 073001.

Agostini, F.; Min, S. K.; Abedi, A.; Gross, E. K. U. *JCTC* **2016**, *12* (5), 2127–2143.

Coupled-trajectory MQC approach (CTMQC)

Coupled trajectory method (CTMQC)

- The quantum momentum calculation

The nuclear density is reproduced by the ensemble of trajectories $\{\boldsymbol{R}^J(t), \boldsymbol{P}^J(t)\}$. It is expressed as Gaussian functions $\{g_{\sigma_\nu^J(t)}\}$ to express the quantum momentum analytically.

$$|\chi^J(t)|^2 = \frac{1}{N_{tr}} \sum_K^{N_{tr}} \prod_\nu g_{\sigma_\nu^K(t)}(R_\nu^J - R_\nu^K(t))$$

$$-i\mathcal{P}_\nu^J = -\hbar \frac{\nabla_\nu |\chi^J|}{|\chi^J|} = -\hbar \frac{\nabla_\nu |\chi^J|^2}{2|\chi^J|^2}$$

$$\mathcal{P}_\nu^J(t) = \sum_K^{N_{tr}} W_\nu^{JK}(t)(R_\nu^J(t) - R_\nu^K(t))$$
$$= \alpha_\nu^J(t) R_\nu^J(t) - R_{0\nu}^J(t)$$

$$W_\nu^{JK} = \frac{\hbar \prod_\mu g_{\sigma_\mu^K(t)}(R_\mu^J(t) - R_\mu^K(t))}{2\sigma_\nu^{K,2}(t) \sum_M \prod_\mu g_{\sigma_\mu^M(t)}(R_\mu^J(t) - R_\mu^M(t))}$$

Thus, the quantum momentum of each trajectory becomes a **linear** function constructed by the slope and y-intercept, which are computed through the trajectory ensemble.

Min, S. K.; Agostini, F.; Tavernelli, I.; Gross, E. K. U. *JPCL.* **2017**, *8* (13), 3048–3055.
Agostini, F.; Min, S. K.; Abedi, A.; Gross, E. K. U. *JCTC.* **2016**, *12* (5), 2127–2143.

Coupled trajectory method (CTMQC)

- TD vector potential calculation

In order to compute the TD vector potential, spatial derivative of the coefficients needs to be approximated.

$\nabla_\nu |C_i^J| \approx 0$ in most of the region

$$C_i^J = |C_i^J| \exp\left(\frac{i}{\hbar}\theta_i^J\right) \Rightarrow \nabla_\nu C_i^J = \left(\frac{\nabla_\nu |C_i^J|}{|C_i^J|} + \frac{i}{\hbar}\theta_i^J\right) C_i^J \approx \frac{i}{\hbar}\theta_i^J C_i^J$$

$$\dot{C}_i^J \approx -\frac{i}{\hbar} E_i^J C_i^J \Rightarrow \frac{d}{dt}|C_i^J| \exp\left(\frac{i}{\hbar}\theta_i^J\right) + \frac{i}{\hbar}\dot{\theta}_i^J C_i^J = -\frac{i}{\hbar} E_i^J C_i^J \Rightarrow \dot{\theta}_i^J = -E_i^J$$

0

$$\Rightarrow \frac{d}{dt}\nabla_\nu \theta_i^J = -\nabla_\nu E_i^J \Rightarrow \phi_{i,\nu}^J(t) = \nabla_\nu \theta_i^J = -\int^t dt' \, \nabla_\nu E_i^J$$

Phase gradient

$$A_\nu^J = \sum_i \rho_{ii}^J \phi_{i,\nu}^J + \hbar \Im \sum_{ij} \rho_{ij}^J d_{ij,\nu}^J$$

cf. adiabatic density matrix

$$\rho_{ij}^J = C_i^J C_j^{*J}$$

Agostini, F.; Min, S. K.; Abedi, A.; Gross, E. K. U. *JCTC.* **2016**, *12* (5), 2127–2143.

Agostini, F.; Abedi, A.; Suzuki, Y.; Min, S. K.; Maitra, N. T.; Gross, E. K. U. *JCP.* **2015**, *142* (8), 084303.

Coupled trajectory method (CTMQC)

- Equations of motion (EOMs)
  - The electron-nuclear correlation beyond the Ehrenfest terms naturally appear in electronic and nuclear EOMs.
  - With the predefined trajectories, electronic and nuclear evolutions are conducted simultaneously. Through the quantum momentum, each trajectory is "connected".

Electronic part

$$\dot{C}_i^K = -\frac{i}{\hbar} E_i^K C_i^K - \sum_j C_j^K \sum_\nu \frac{P_\nu^K}{M_\nu} \cdot d_{ij,\nu}^K + \sum_\nu \frac{i\mathcal{P}_\nu^K}{\hbar M_\nu} \cdot \left(\sum_j \left| C_j^K \right|^2 \phi_{j\nu}^K - \phi_{i\nu}^K \right) C_i^K$$

Nuclear part

$$F_\nu^K = -\sum_i \rho_{ii}^K \nabla_\nu E_i^K - \sum_{ij} \rho_{ij}^K \left(E_j^K - E_i^K \right) d_{ij,\nu}^K + \sum_i \rho_{ii}^K \left(\sum_\mu \frac{2i\mathcal{P}_\mu^K}{\hbar M_\mu} \cdot \phi_{i,\mu}^K \right) \left(\sum_j \rho_{jj}^K \phi_{j,\nu}^K - \phi_{i,\nu}^K \right)$$

Agostini, F.; Min, S. K.; Abedi, A.; Gross, E. K. U. *JCTC.* **2016**, *12* (5), 2127–2143.

Coupled trajectory method (CTMQC)

- New electron-nuclear correlation compared to Ehrenfest/Surface hopping dynamics
  - A swarm of trajectories are propagated to construct nuclear quantum momentum
  - The phase gradients from adiabatic forces
  - Wavepacket splitting and (de)coherence are properly captured in the model Hamiltonian simulations.

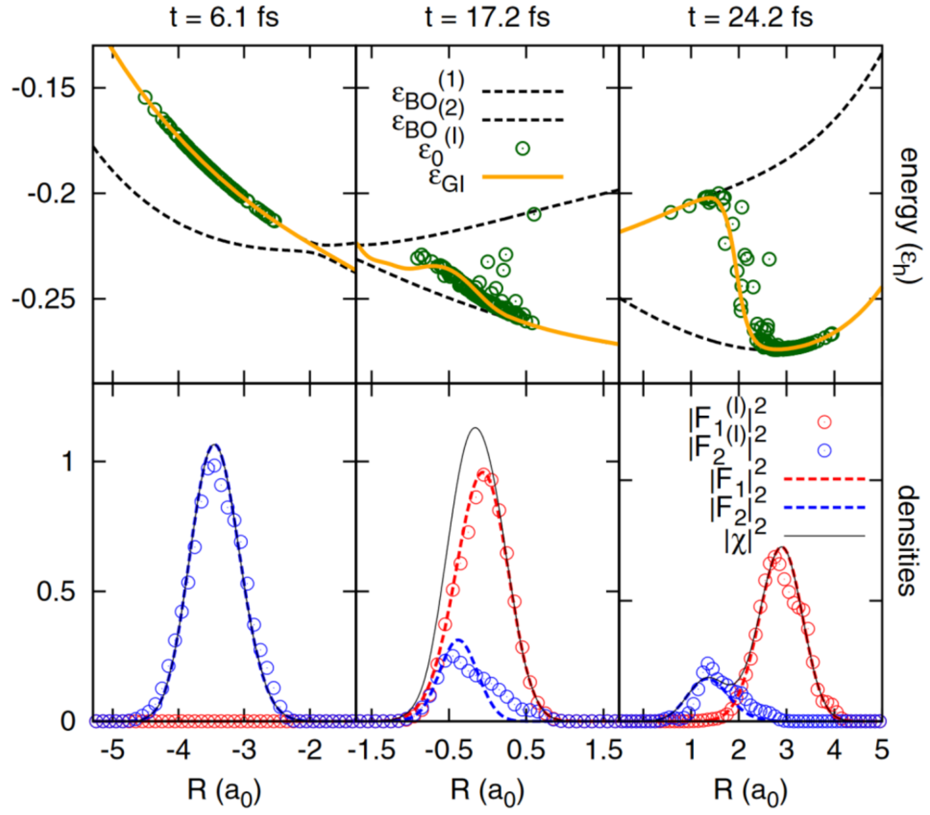

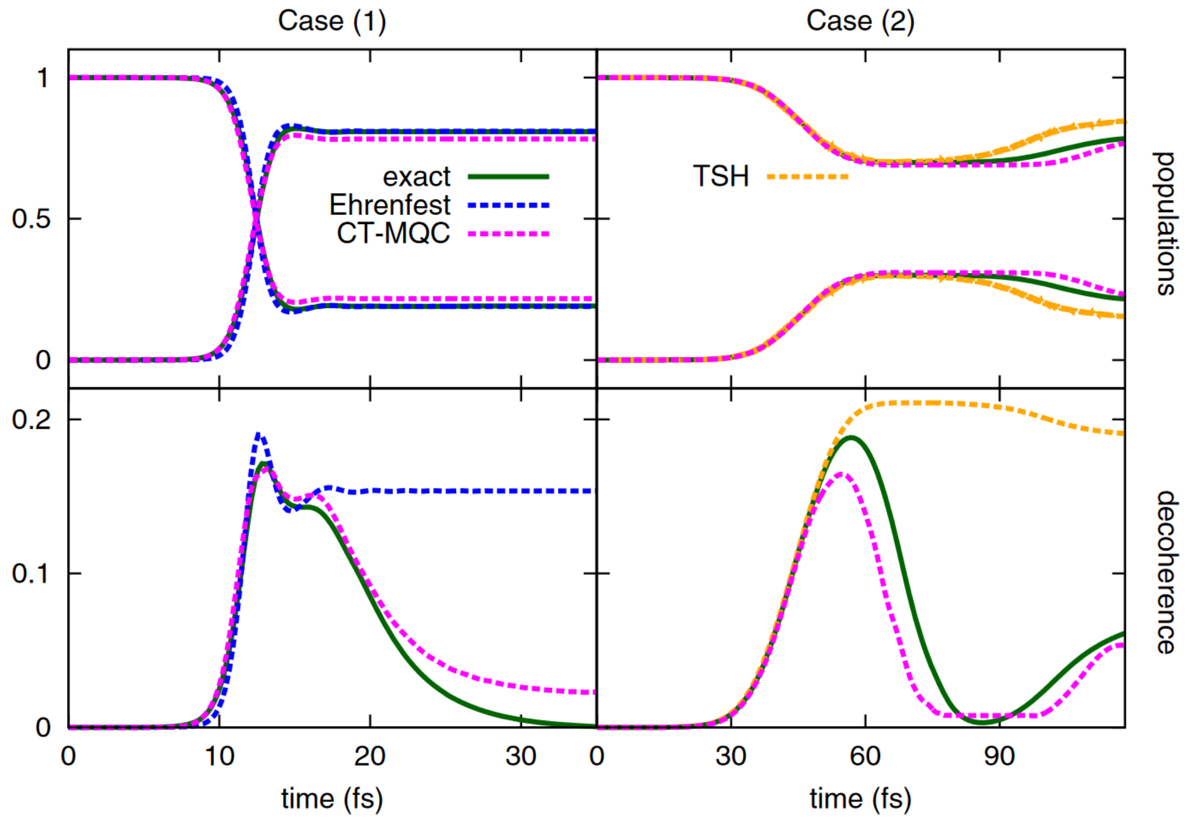

Min, S. K.; Agostini, F.; Gross, E. K. U. *PRL* **2015**, *115* (7), 073001.

Coupled trajectory method (CTMQC)

- Applications to the molecular systems

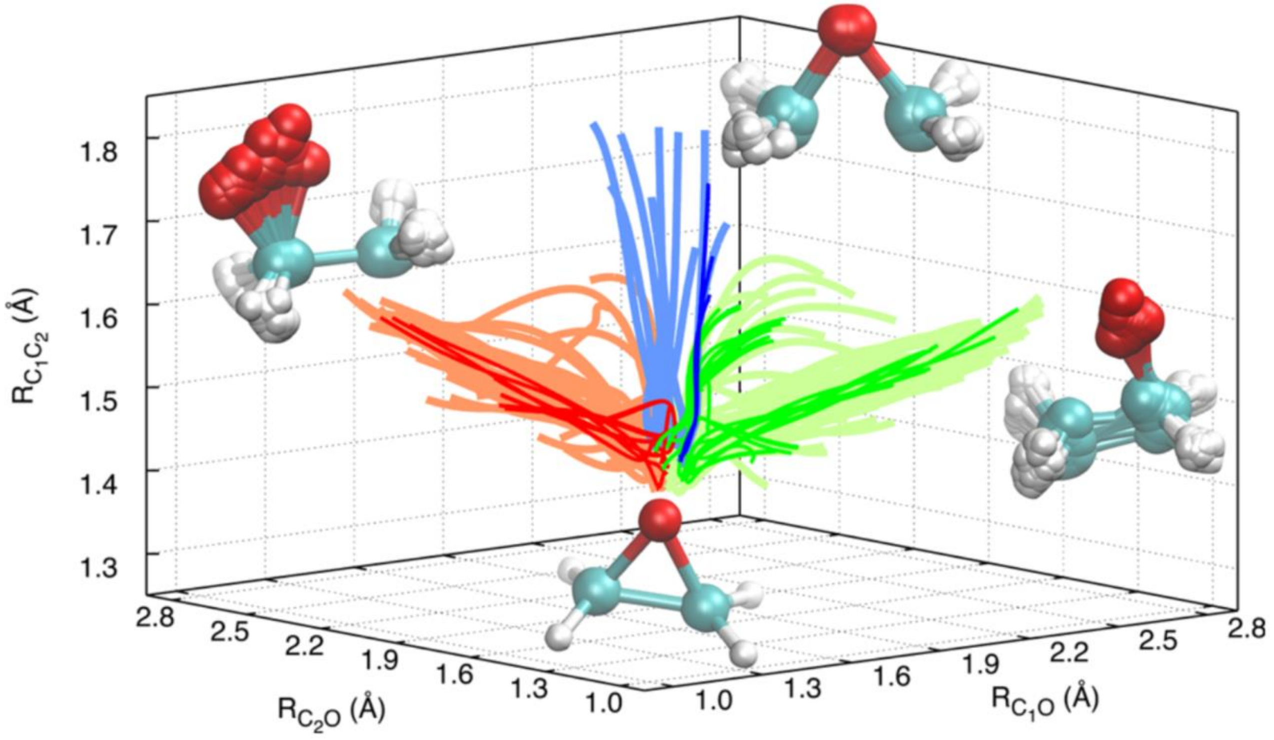

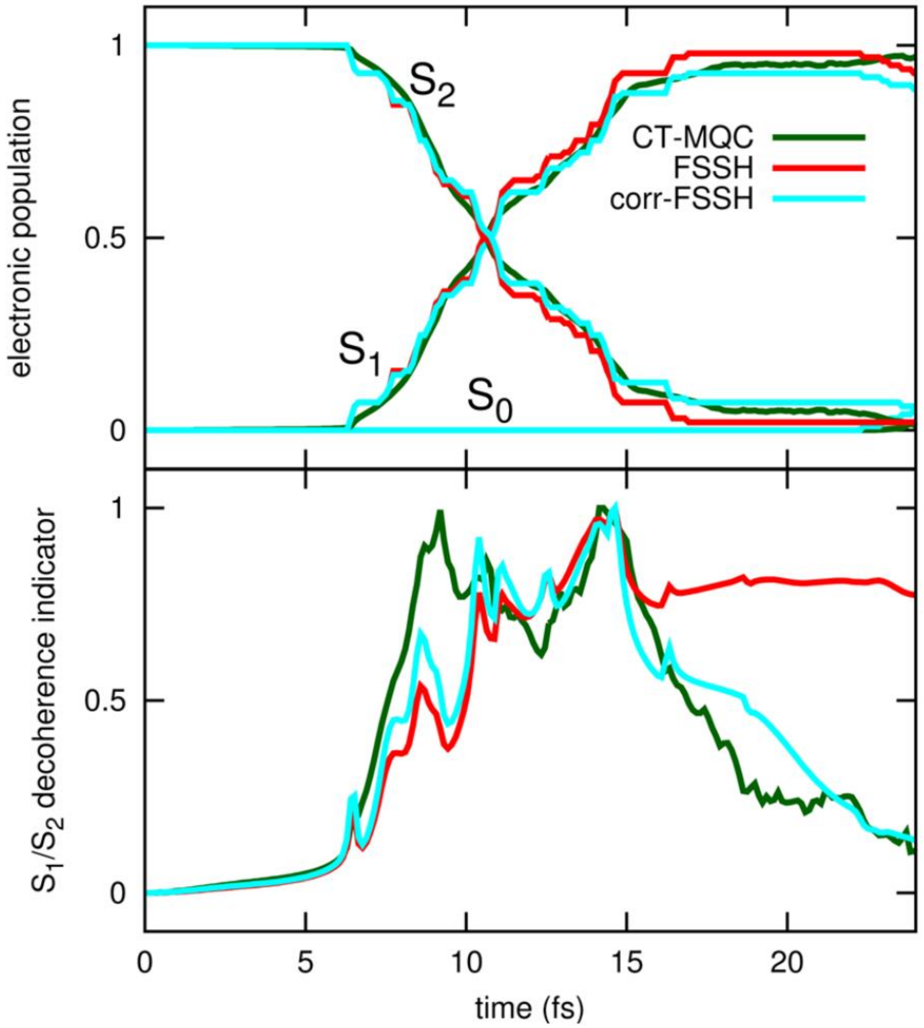

Photochemistry of Oxirane; excited-state calculation with LR-TDDFT

Min, S. K.; Agostini, F.; Tavernelli, I.; Gross, E. K. U. *JPCL.* **2017**, *8* (13), 3048–3055.

Coupled trajectory method (CTMQC)

- More works…

Energy conservation through modifying the phase gradient calculation (CTMQC-E)

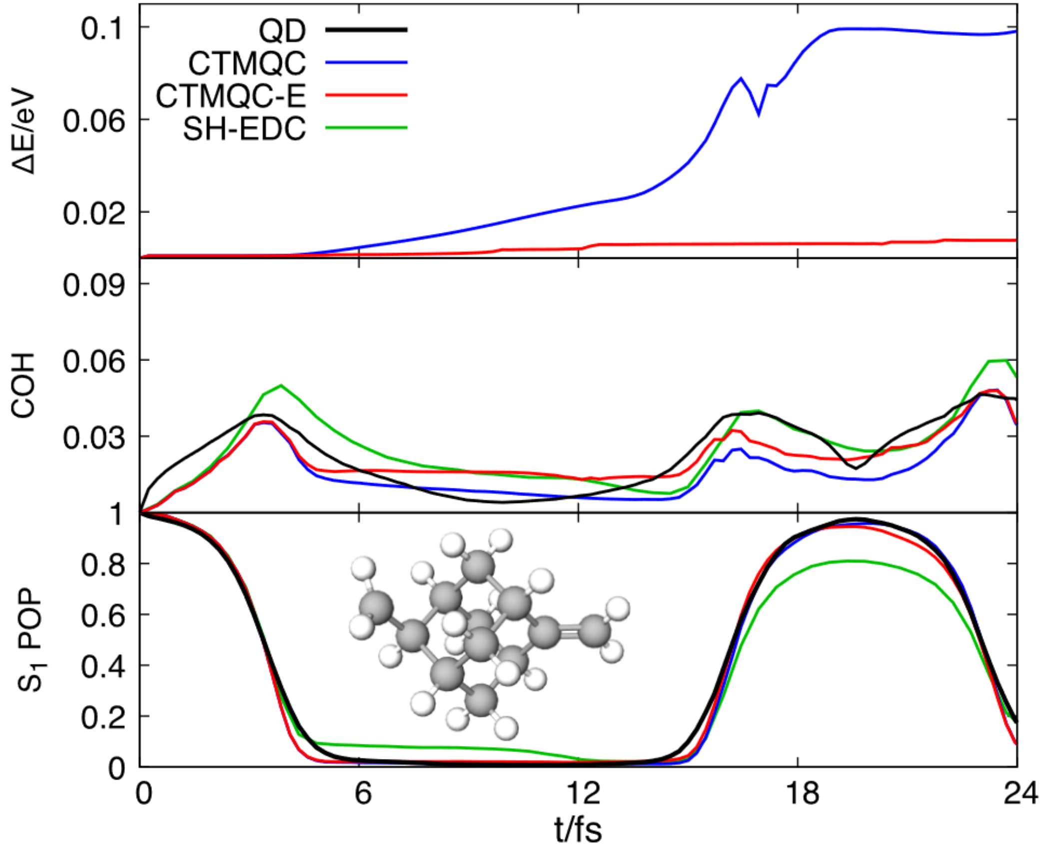

Arribas, E. V.; Ibele, L. M.; Lauvergnat, D.; Maitra, N. T.; Agostini, F. *JCTC.* **2023**, *19* (21), 7787–7800.

Simplified nuclear dynamics based on TSH (CTSH)

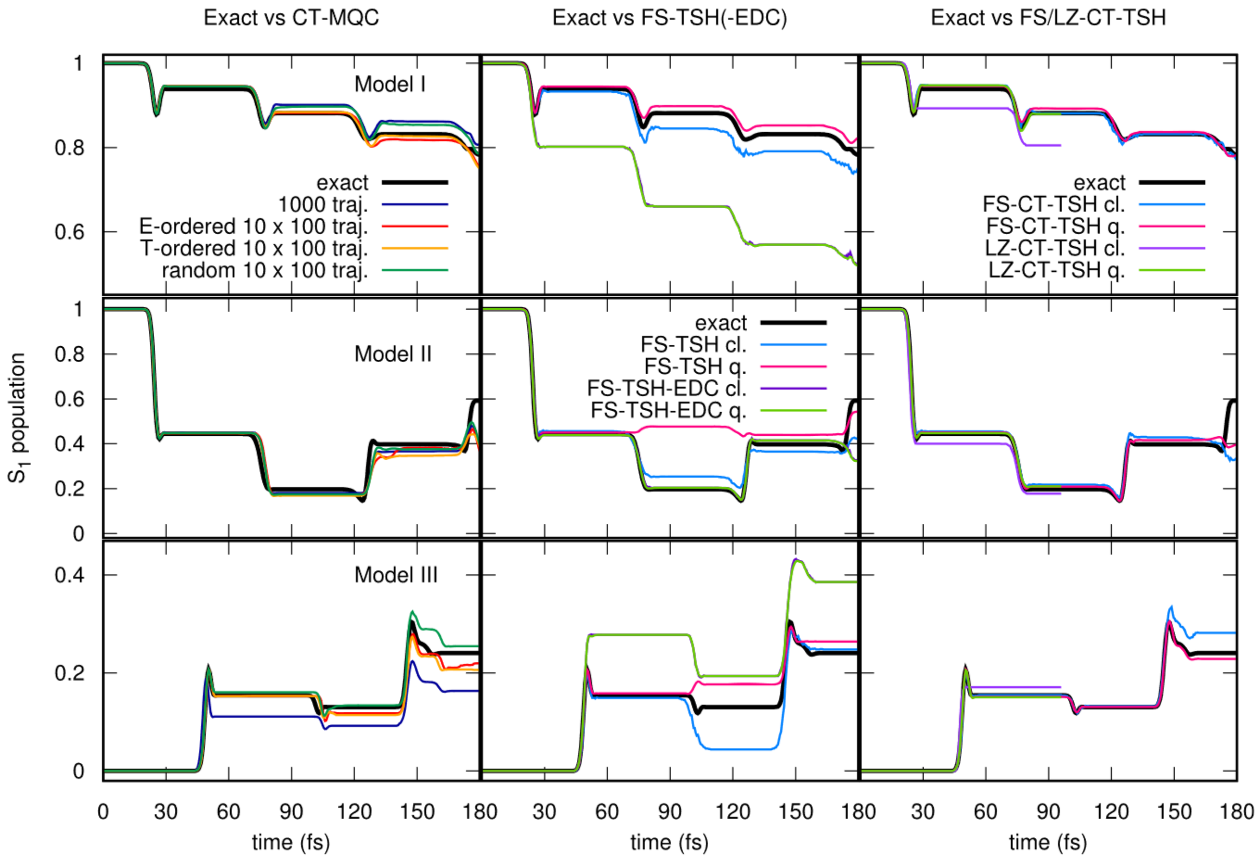

Pieroni, C.; Agostini, F. *JCTC.* **2021**, *17* (10), 5969–5991.

Independent-trajectory XF methods

Necessity of the independent-trajectory algorithm

- The CTMQC algorithm is efficient, but it requires more cost than that in the conventional TSH method.
  - Simultaneous propagation of a swarm of trajectories
  - The NACV calculation for computing the decoherence force

- The stability of the CTMQC calculation is sensitive to the excited-state calculation in each trajectory (Excited-state calculations need to be stable for all trajectories).

⬇

How can we simplify the force so that explicit NACV calculation is not obliged?

How to define the quantum momentum in the level of independent trajectory?

Surface hopping based on XF (SHXF)

- Nuclear EOM: Based on the FSSH force, that is, the adiabatic force of an active state determined by the hopping process is employed to evolve nuclei.

$$P_{i\to j} = \frac{2\Re\left(\rho_{ij}\sum_\nu \dot{R}_\nu \cdot d_{ij,\nu}\right)}{\rho_{ii}}\,\Delta t$$

- Electronic EOM: Only electronic propagation contains the decoherence term.

$$\dot{C}_i = -\frac{i}{\hbar}E_i C_i - \sum_j C_j \sum_\nu \frac{P_\nu}{M_\nu}\cdot d_{ij,\nu} + \sum_\nu \frac{i\mathcal{P}_\nu}{\hbar M_\nu}\cdot\left(\sum_j |C_j|^2 \phi_{j\nu} - \phi_{i\nu}\right) C_i$$

- To compute the quantum momentum in the independent-trajectory level, auxiliary trajectories are employed for each trajectory to estimate the overall nuclear wavepacket distribution.

Ha, J.-K.; Lee, I. S.; Min, S. K. *JPCL.* **2018**, *9* (5), 1097–1104.

Agostini, F.; Min, S. K.; Abedi, A.; Gross, E. K. U. *JCTC.* **2016**, *12* (5), 2127–2143.

Surface hopping based on XF (SHXF)

- Auxiliary trajectory propagation
  - When the coherence criterion, that is, $\epsilon < |C_i|^2 < 1 - \epsilon$, are satisfied for a state, the auxiliary trajectory is spawned for that state.
  - The initial aux. position $\boldsymbol{R}_i$ is set to the real position at the spawning time t_i.

$$\boldsymbol{R}_i(t_i) = \boldsymbol{R}(t_i)$$

  - The aux. momentum $\boldsymbol{P}_i$ is set by rescaling $\boldsymbol{P}_i = \alpha_i \boldsymbol{P}$ based on the energy conservation.

$$\frac{1}{2}\boldsymbol{P}_i^T \boldsymbol{M}^{-1} \boldsymbol{P}_i + E_i = \frac{1}{2}\boldsymbol{P}^T \boldsymbol{M}^{-1} \boldsymbol{P} + E$$

  - The aux. position is propagated by the current aux. momentum.

$$\boldsymbol{R}_i(t + \Delta t) = \boldsymbol{R}_i(t) + \boldsymbol{M}^{-1} \boldsymbol{P}_i(t) \Delta t$$

  - When the coherence criterion is no longer satisfied, or a hop occurs, aux. trajectories are destroyed.

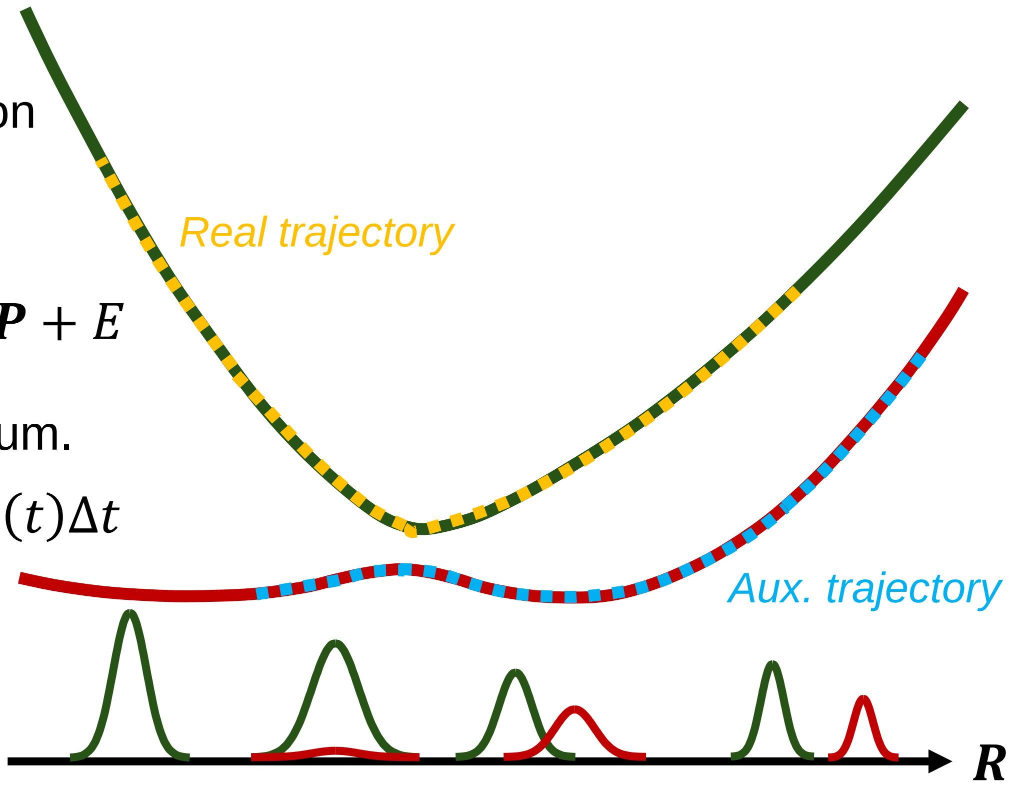

Ha, J.-K.; Lee, I. S.; Min, S. K. *JPCL.* **2018**, *9* (5), 1097–1104.

Surface hopping based on XF (SHXF)

- Quantum momentum

The nuclear density is assumed to be combination of Gaussian functions having each aux. position as its center.

$$|\chi|^2 = \sum_i |\chi_i|^2 = \sum_i N_i \prod_\nu \exp\left(-\frac{\left(R_\nu - R_{i,\nu}\right)^2}{2\sigma_{i,\nu}^2}\right)$$

⬇

$$\mathcal{P}_\nu \approx \frac{i\hbar}{2\sigma_\nu^2}\left(R - \langle R_\nu \rangle\right) \approx \frac{i\hbar}{2\sigma_\nu^2}\left(R_{a,\nu} - \sum_i \rho_{ii} R_{i,\nu}\right)$$

Eventually, the sign of quantum momentum is determined by the displacement between the real position and average position. By this procedure, each trajectory possesses its own quantum momentum constructed by its auxiliary trajectories.

Ha, J.-K.; Lee, I. S.; Min, S. K. *JPCL.* **2018**, *9* (5), 1097–1104.

Surface hopping based on XF (SHXF)

- Phase gradient

The phase gradient is computed by the momentum difference during the coherence.

$$\phi_{i,\nu} = -\int_{t_i}^{t} dt' \, \nabla_\nu E_i = \int_{t_i}^{t} dt' \, F_i = \int_{t_i}^{t} dP_i$$

⬇

$$\phi_{i,\nu}(t) = P_i(t) - P_i(t_i)$$

Thus, quantum momentum and phase gradient become physical quantities in terms of the relative position and momentum.

Ha, J.-K.; Lee, I. S.; Min, S. K. *JPCL.* **2018**, *9* (5), 1097–1104.

Surface hopping based on XF (SHXF)

- Decoherence correction through the electron-nuclear correlation term

The newly deduced electron-nuclear correlation contribution to the density is the following.

$$\dot{\rho}_{ii}^{XF} = \sum_{\nu} \frac{2i\mathcal{P}_{\nu}}{M_{\nu}} \cdot \sum_{j} (\phi_{j,\nu} - \phi_{i,\nu}) \rho_{jj} \rho_{ii}$$

⬇

$$\dot{\rho}_{ii}^{XF} = -\sum_{\nu} \frac{\hbar}{M_{\nu}\sigma_{\nu}} \boxed{(R_{\nu} - \langle R_{\nu} \rangle)} \cdot \boxed{\sum_{j} (\phi_{j,\nu} - \phi_{i,\nu})} \rho_{jj} \rho_{ii}$$

The direction of the decoherence is determined by the interplay between the relative position and momentum.

Ha, J.-K.; Lee, I. S.; Min, S. K. *JPCL.* **2018**, *9* (5), 1097–1104.

Surface hopping based on XF (SHXF)

- Auxiliary trajectory propagation & decoherence correction

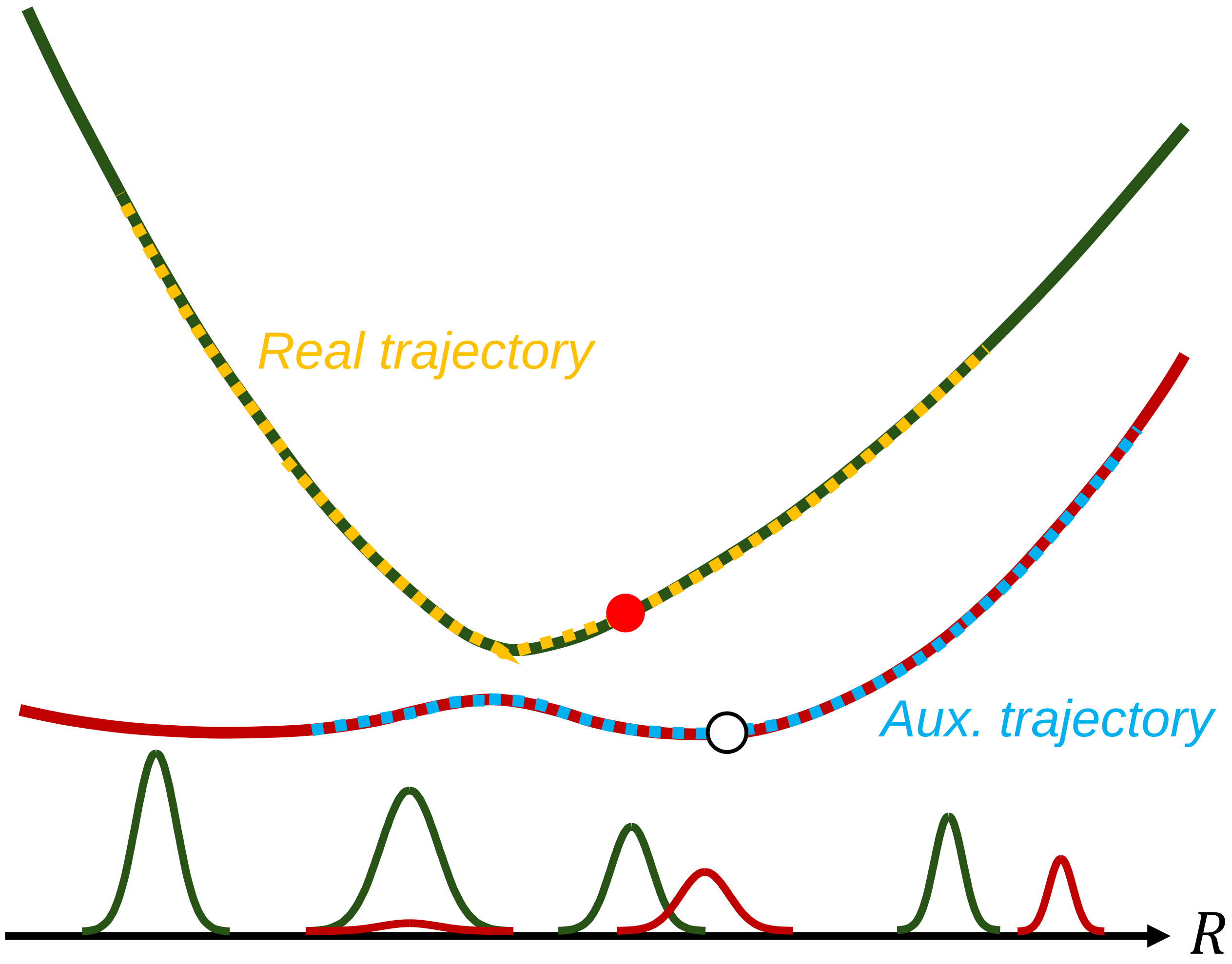

$$\dot{\rho}_{00}^{XF} = -\frac{\hbar}{M\sigma}\underbrace{(R - \langle R \rangle)}_{<0} \cdot \overbrace{(\phi_1 - \phi_0)}^{<0}\rho_{11}\rho_{00}$$

$$\dot{\rho}_{11}^{XF} = -\frac{\hbar}{M\sigma}\underbrace{(R - \langle R \rangle)}_{<0} \cdot \underbrace{(\phi_0 - \phi_1)}_{>0}\rho_{00}\rho_{11}$$

The electron-nuclear correlation acts as the decoherence correction, increasing ρ_{11} and decreasing ρ_{00}.

Ha, J.-K.; Lee, I. S.; Min, S. K. *JPCL.* **2018**, *9* (5), 1097–1104.

Surface hopping based on XF (SHXF)

- Auxiliary trajectory propagation & decoherence correction

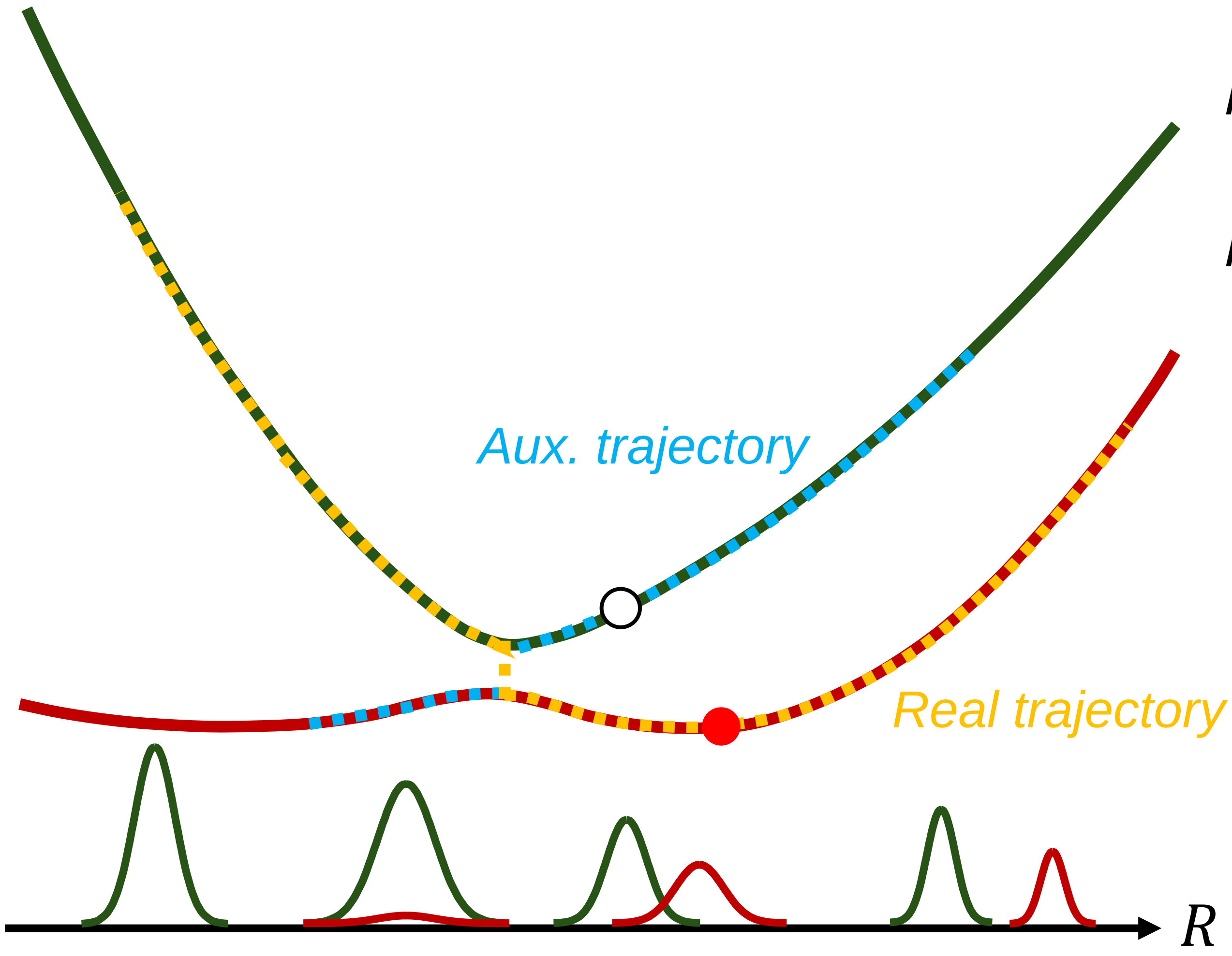

$$\dot{\rho}_{00}^{XF} = -\frac{\hbar}{M\sigma}\underbrace{(R - \langle R \rangle)}_{>0} \cdot \overbrace{(\phi_1 - \phi_0)}^{<0}\rho_{11}\rho_{00}$$

$$\dot{\rho}_{11}^{XF} = -\frac{\hbar}{M\sigma}\underbrace{(R - \langle R \rangle)}_{>0} \cdot \underbrace{(\phi_0 - \phi_1)}_{>0}\rho_{00}\rho_{11}$$

The electron-nuclear correlation acts as the decoherence correction, increasing ρ_{00} and decreasing ρ_{11}.

Decoherence facilitates the population transfer to the active state → The active state serves as the pointer state!

Ha, J.-K.; Lee, I. S.; Min, S. K. *JPCL.* **2018**, *9* (5), 1097–1104.

Shu, Y.; Truhlar, D. G. *JCTC.* **2023**, *19* (2), 380–395.

Surface hopping based on XF (SHXF)

- Branching correction on the auxiliary trajectory propagation

When the dynamics encounters the classical turning point, there are some difficulties for defining the auxiliary momenta

Case I. An auxiliary trajectory encounters the turning point.

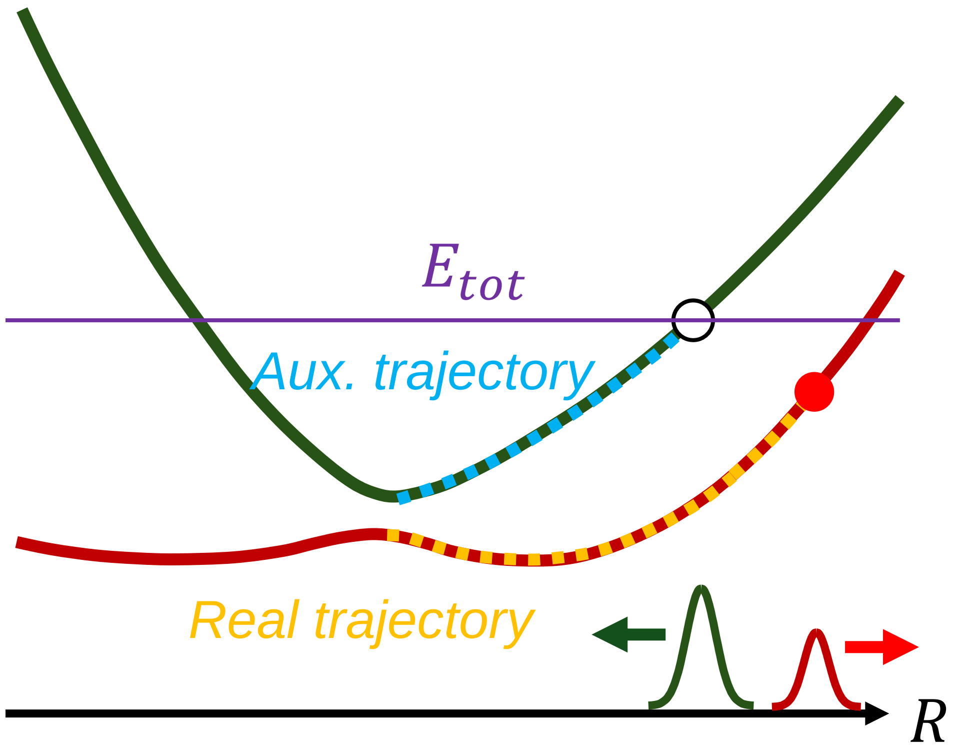

In this case, the auxiliary trajectory needs to reflect. However, the aux. momentum is computed by the positive scaling of the real momentum. Thus, a special treatment is necessary.

$$\boldsymbol{P}_i = \alpha_i(> 0)\boldsymbol{P}$$

Inspired by the BCSH method, one can the density of the auxiliary state and initialize the auxiliary project out trajectory.

Arribas, E. V.; Vindel-Zandbergen, P.; Roy, S.; Maitra, N. T. *PCCP.* **2023**, *25* (38), 26380–26395.

Xu, J.; Wang, L. *JCP.* **2019**, *150* (16), 164101.

Surface hopping based on XF (SHXF)

- Branching correction on the auxiliary trajectory propagation

When the dynamics encounters the classical turning point, there are some difficulties for defining the auxiliary momenta

Case II. The real trajectory encounters the turning point.

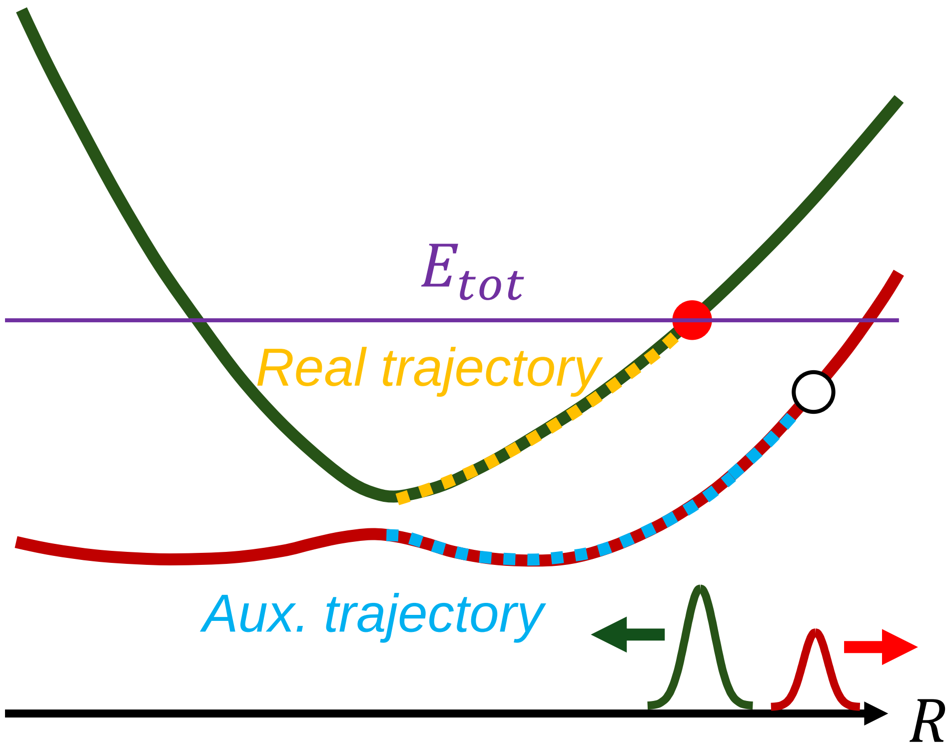

In this case, the auxiliary trajectory would experience abrupt momentum reversal, which could cause a wrong decoherence correction.

Here, one can collapse the state to the active state. The criterion for the turning point is based on the BCSH turning point descriptor.

$$\boldsymbol{F}^T(t+\Delta t)\boldsymbol{P}_i(t+\Delta t)\cdot\boldsymbol{F}^T(t+\Delta t)\boldsymbol{P}_i(t) < 0 \;\Rightarrow\; \textit{turning point}$$

Ha, J.-K.; Min, S. K. *JCP.* **2022**, *156* (17), 174109.
Xu, J.; Wang, L. *JCP.* **2019**, *150* (16), 164101.

Surface hopping based on XF (SHXF)

- Independent-trajectory MQC approach based on TSH
  - Proper description of multiple crossing in the NaI pump-probe experiment modeling
  - Excited-state dynamics of $CH_2NH_2^+$ at ambient temperature ($S_2 \rightarrow S_1 \rightarrow S_0$)

NaI Hamiltonian

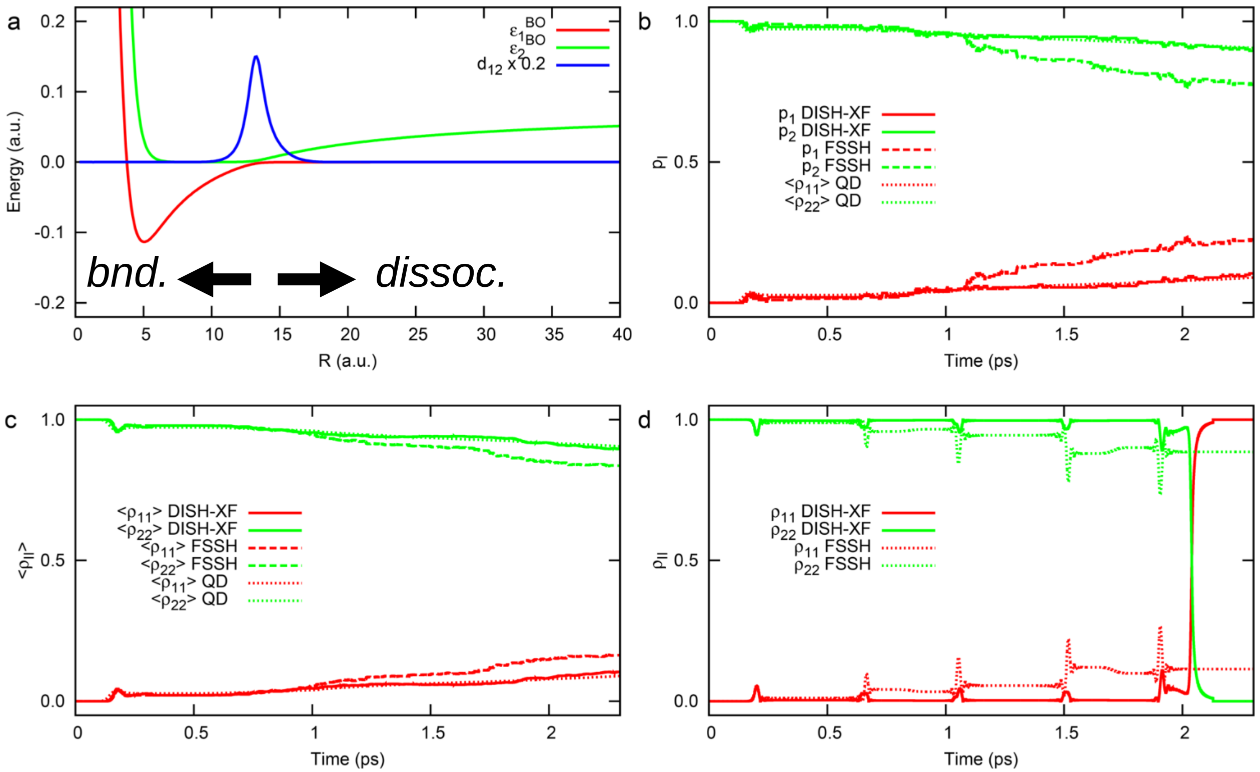

Photochemistry of $CH_2NH_2^+$

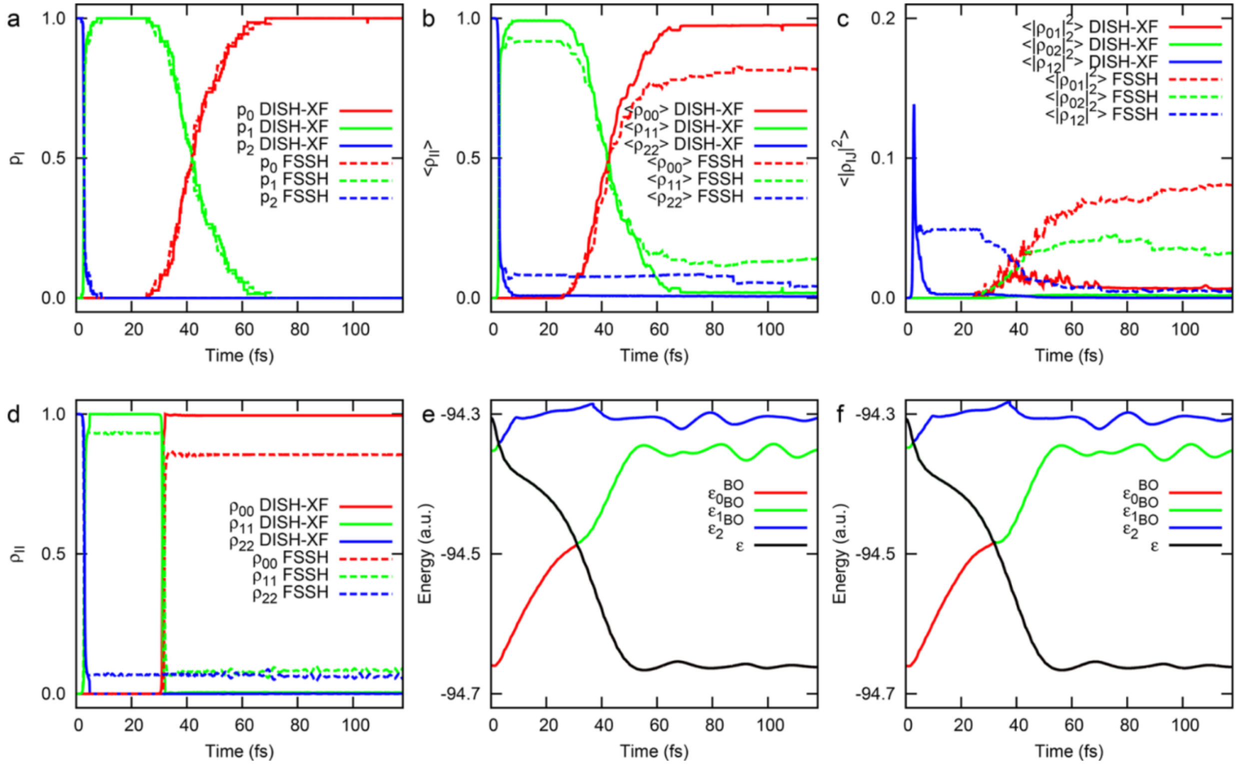

Ha, J.-K.; Lee, I. S.; Min, S. K. *JPCL.* **2018**, *9* (5), 1097–1104.

Surface hopping based on XF (SHXF)

- Applications to the molecular systems

Photoisomerization of molecular rotors

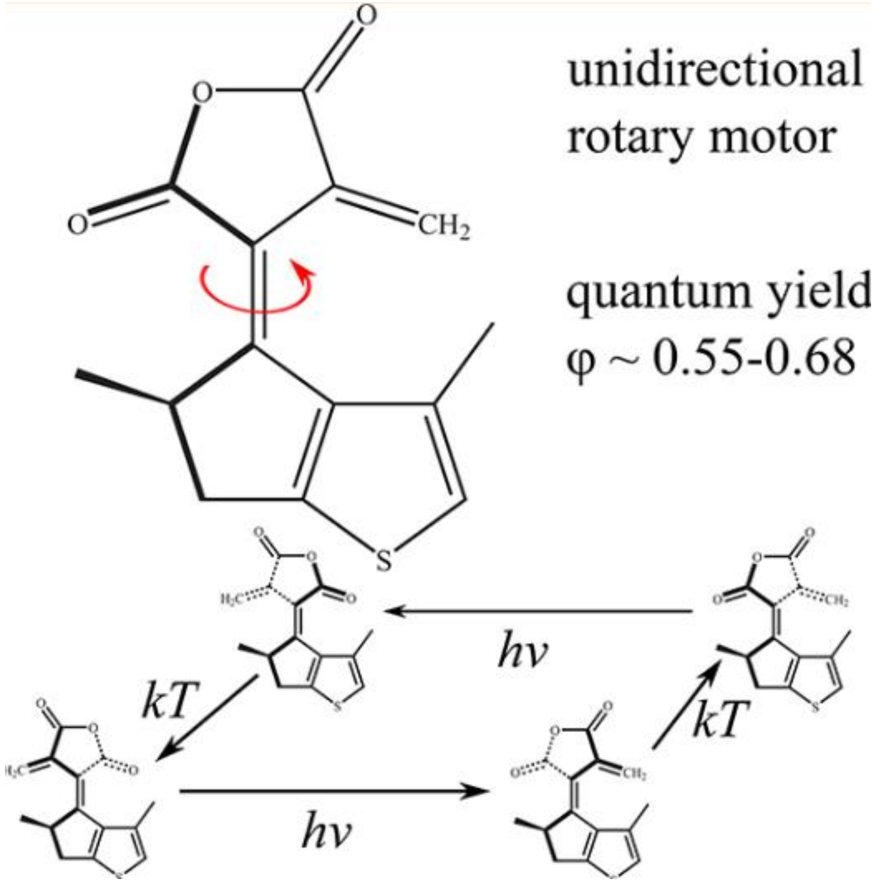

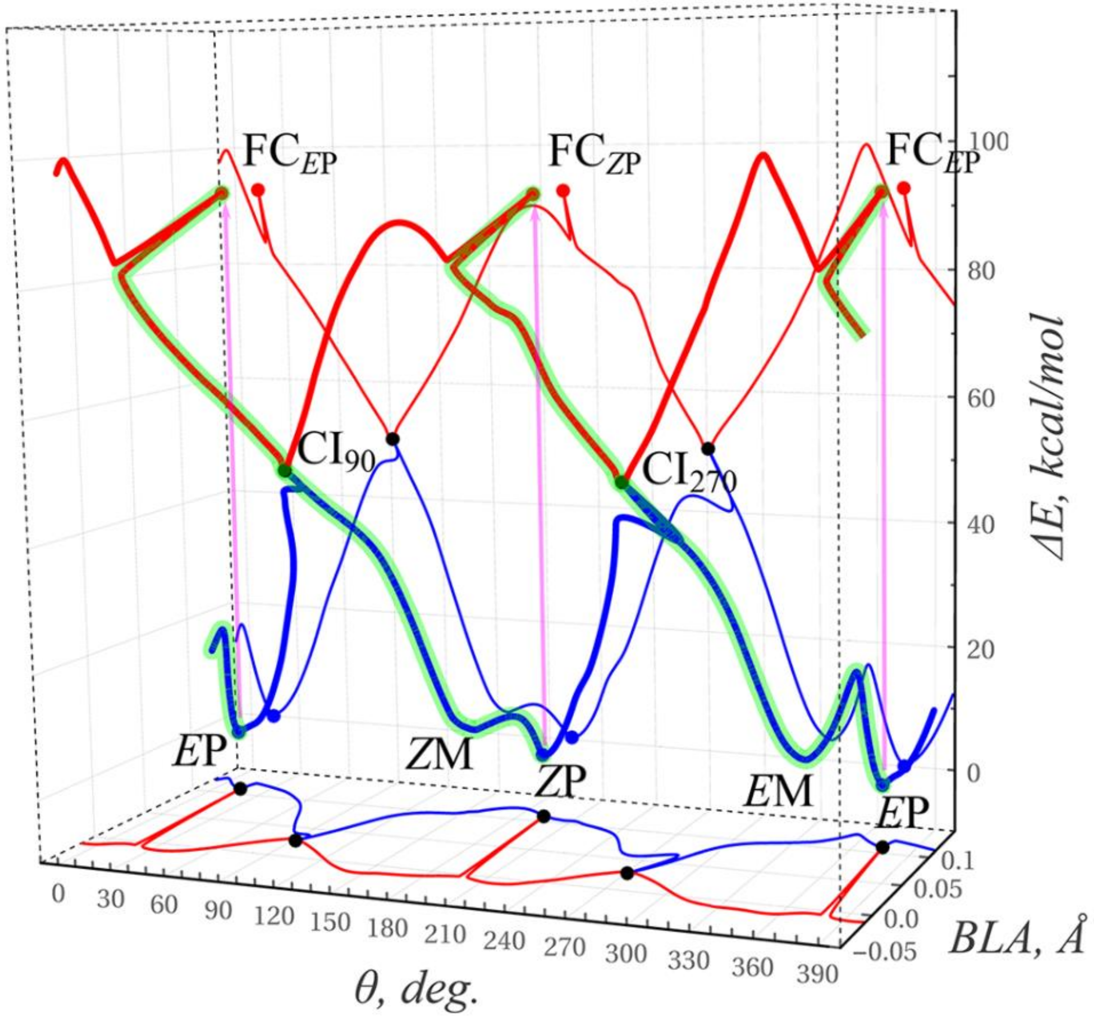

Filatov, M.; Paolino, M.; Min, S. K.; Kim, K. S. *JPCL*. **2018**, *9* (17), 4995–5001.

Surface hopping based on XF (SHXF)

- More works…

Study on multistate crossing through the LVC model of an uracil cation with SHXF

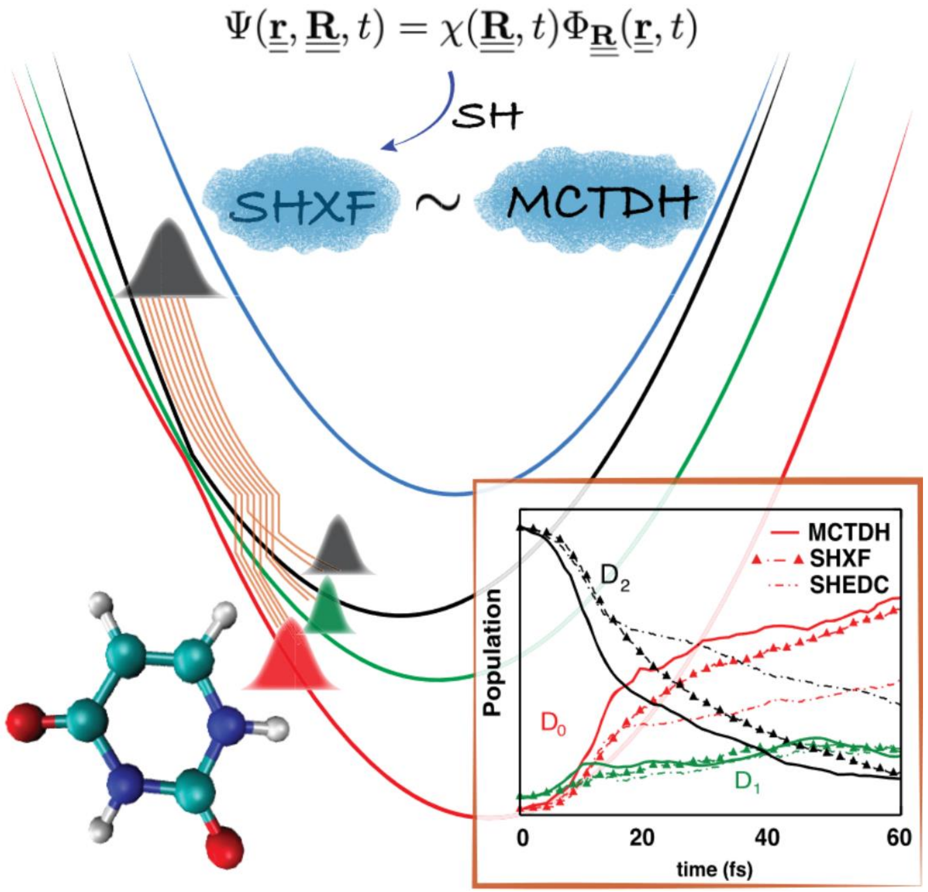

Overall review of the independent-trajectory XF methods including SHXF

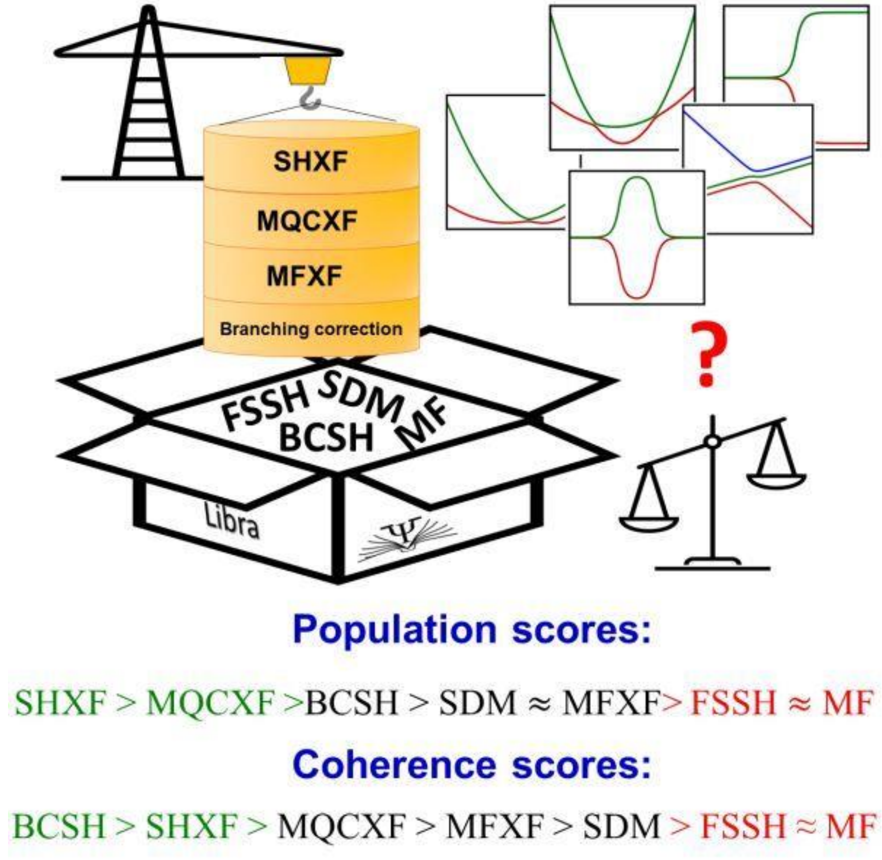

Vindel-Zandbergen, P.; Matsika, S.; Maitra, N. T. *JPCL.* **2022**, *13* (7), 1785–1790.

Han, D.; Akimov, A. V. *JCTC.* **2024**, *20* (12), 5022–5042.

Mixed quantum-classical based on XF (MQCXF)

- Recovery of the decoherence force in the independent-trajectory XF method

How about employing the decoherence force derived in the CTMQC equations as well in the independent-trajectory level?

$$\dot{C}_i = -\frac{i}{\hbar}E_i C_i - \sum_j C_j \sum_\nu \frac{P_\nu}{M_\nu} \cdot d_{ij,\nu} + \sum_\nu \frac{i\mathcal{P}_\nu}{\hbar M_\nu} \cdot \left(\sum_j |C_j|^2 \phi_{j\nu} - \phi_{i\nu} \right) C_i$$

$$F_\nu = -\sum_i \rho_{ii} \nabla_\nu E_i - \sum_{ij} \rho_{ij} \left(E_j - E_i \right) d_{ij,\nu} + \sum_{ij} \rho_{ii}\rho_{jj} \left[\sum_\mu \frac{2i\mathcal{P}_\mu}{\hbar M_\mu} \cdot \left(\phi_{j,\mu} - \phi_{i,\mu} \right) \right] \phi_{i,\nu}$$

However, for more reliable results, the energy conservation of the XF force needs to be addressed.

Ha, J.-K.; Min, S. K. *JCP.* **2022**, *156* (17), 174109.

Mixed quantum-classical based on XF (MQCXF)

- Modified phase gradient calculation

For the energy conservation, the modified phase gradient is utilized in MQCXF.

$$\dot{E}_{tot} = \sum_{\nu} F_{\nu} \cdot \dot{R}_{\nu} + \sum_{i} \left(\dot{\rho}_{ii} E_i + \rho_{ii} \sum_{\nu} \nabla_{\nu} E_i \cdot \dot{R}_{\nu} \right)$$

$$= \sum_{ij} \rho_{ii}\rho_{jj} \left[\sum_{\mu} \frac{\mathcal{P}_{\mu}}{\hbar M_{\mu}} \cdot \left(\phi_{i,\mu} - \phi_{j,\mu} \right) \right] \left[E_i - E_j + \sum_{\nu} \left(\phi_{i,\nu} - \phi_{j,\nu} \right) \cdot \dot{R}_{\nu} \right] \overset{!}{=} 0$$

$$\Rightarrow \quad E_i - E_j + \sum_{\nu} \left(\phi_{i,\nu} - \phi_{j,\nu} \right) \cdot \dot{R}_{\nu} = 0 \quad \Rightarrow \quad \phi_{i,\nu} - \phi_{j,\nu} = -\frac{E_i - E_j}{\sum_{\nu} n_{\nu} \cdot \dot{R}_{\nu}} n_{\nu}$$

$$\Rightarrow \quad \boxed{\phi_{i,\nu} - \phi_{j,\nu} = -\frac{E_i - E_j}{2E_{kin}} P_{\nu}}$$

$n_{\nu} := P_{\nu}$

The energy-based phase approximation

Ha, J.-K.; Min, S. K. *JCP.* **2022**, *156* (17), 174109.

Time-dependent Gaussian widths

- Time-dependent Gaussian width approximations

It is likely that the nuclear wavepacket width would change during the dynamics. In order to consider those change in the quantum momentum calculation, one may apply the time-dependent width.

- Schwartz scheme [Bedard-Hearn, M. J.; Larsen, R. E.; Schwartz, B. J. *JCP.* **2005**, 123 (23), 234106.]

$$\sigma_\nu^{-2}(t) = \left(\frac{(w_\nu/\mathrm{Bohr})^2}{2\lambda_{D,\nu}(t)}\right)^2 = \left(\frac{(w_\nu/\mathrm{Bohr})^2 P_\nu}{4\pi\hbar}\right)^2$$

- Subotnik scheme [Subotnik, J. E. *JPCA.* **2011**, 115 (44), 12083–12096.]

$$\sigma_{ij,\nu}^{-2}(t) = \hbar \frac{|R_{i,\nu} - R_{j,\nu}|}{|P_{i,\nu} - P_{j,\nu}|}$$

Ha, J.-K.; Min, S. K. *JCP.* **2022**, *156* (17), 174109.
Han, D.; Akimov, A. V. *JCTC.* **2024**, *20* (12), 5022–5042.

Implementation of the XF methods in Libra

The XF methods in Libra

- Libra provides SHXF, MQCXF and MFXF (neglect of the XF force in MQCXF).
  - Phase gradient calculation is computed by the momentum difference in SHXF, and by the energy-based approximation in MQCXF and MFXF.
  - Options for addressing the turning points in the auxiliary propagation such the branching correction and other heuristics.
  - Various Gaussian widths approximations including the DOF-resolved width and td width such as Schwartz and Subotnik's.

<table>
<tr><th>Method</th><th>Electronic EOM</th><th>Nuclear force</th><th>Velocity rescaling after a hop</th><th>Energy conservation</th></tr>
<tr><td>SHXF</td><td rowspan="3">$H_{BO} + H_{XF}$</td><td>Active-state force</td><td>Yes</td><td rowspan="2">Yes</td></tr>
<tr><td>MQCXF</td><td>$F_{MF} + F_{XF}$</td><td rowspan="2">No</td></tr>
<tr><td>MFXF</td><td>F_{MF}</td><td>No</td></tr>
</table>

Han, D.; Akimov, A. V. *JCTC.* **2024**, *20* (12), 5022–5042.

The XF methods in Libra

- Electronic propagation in the local diabatization

Under the XF ansatz

$$i\hbar|\Phi_{\boldsymbol{R}}(t)\rangle = [\hat{H}_{BO}\big(\boldsymbol{R}(t)\big) + \hat{H}_{XF}(\boldsymbol{R},t)]|\Phi_{\boldsymbol{R}}(t)\rangle$$

$$|\Psi(\boldsymbol{R},t)\rangle = \chi(\boldsymbol{R},t)|\Phi_{\boldsymbol{R}}(t)\rangle$$

$$\hat{H}_{XF} = -\boldsymbol{\mathcal{P}}^T\boldsymbol{M}^{-1}[\boldsymbol{A} + i\hbar\boldsymbol{\nabla}] = -i\hbar\boldsymbol{\mathcal{P}}^T\boldsymbol{M}^{-1}[|\boldsymbol{\nabla}\Phi_{\boldsymbol{R}}\rangle\langle\Phi_{\boldsymbol{R}}| + |\Phi_{\boldsymbol{R}}\rangle\langle\boldsymbol{\nabla}\Phi_{\boldsymbol{R}}|]$$

[Han, D.; Ha, J.-K.; Min, *JCTC.* **2023**, *19* (8), 2186–2197.]

Applying the Trotter splitting approach within the generalized local diabatization scheme,

Shakiba, M.; Akimov, A. V. *Theor. Chem. Acc.* **2023**, *142* (8), 68.

Granucci, G.; Persico, M.; Toniolo, A. *JCP.* **2001**, *114* (24), 10608–10615.

$$\boldsymbol{C}' = \boldsymbol{U}_{XF}\left(\boldsymbol{C}(t);\frac{\Delta t}{2}\right)\boldsymbol{C}(t)$$

$$\boldsymbol{C}'' = \boldsymbol{T}\boldsymbol{U}_{MF}(\Delta t)\boldsymbol{C}'$$

$$\boldsymbol{C}(t+\Delta t) = \boldsymbol{U}_{XF}\left(\boldsymbol{C}'';\frac{\Delta t}{2}\right)\boldsymbol{C}'$$

$$\boldsymbol{U}_{MF}(\Delta t) = \exp\left(-i\frac{\boldsymbol{H}_{BO}(t) + \boldsymbol{T}^{+}\boldsymbol{H}_{BO}(t+\Delta t)\boldsymbol{T}}{2\hbar}\Delta t\right)$$

$$\boldsymbol{U}_{XF}(\boldsymbol{C}(t);\Delta t) = \exp\left(-i\frac{\boldsymbol{H}_{XF}(\boldsymbol{C}(t))}{2\hbar}\Delta t\right)$$

Han, D.; Akimov, A. V. *JCTC.* **2024**, *20* (12), 5022–5042.

The XF methods in Libra

- Schematics and flowchart

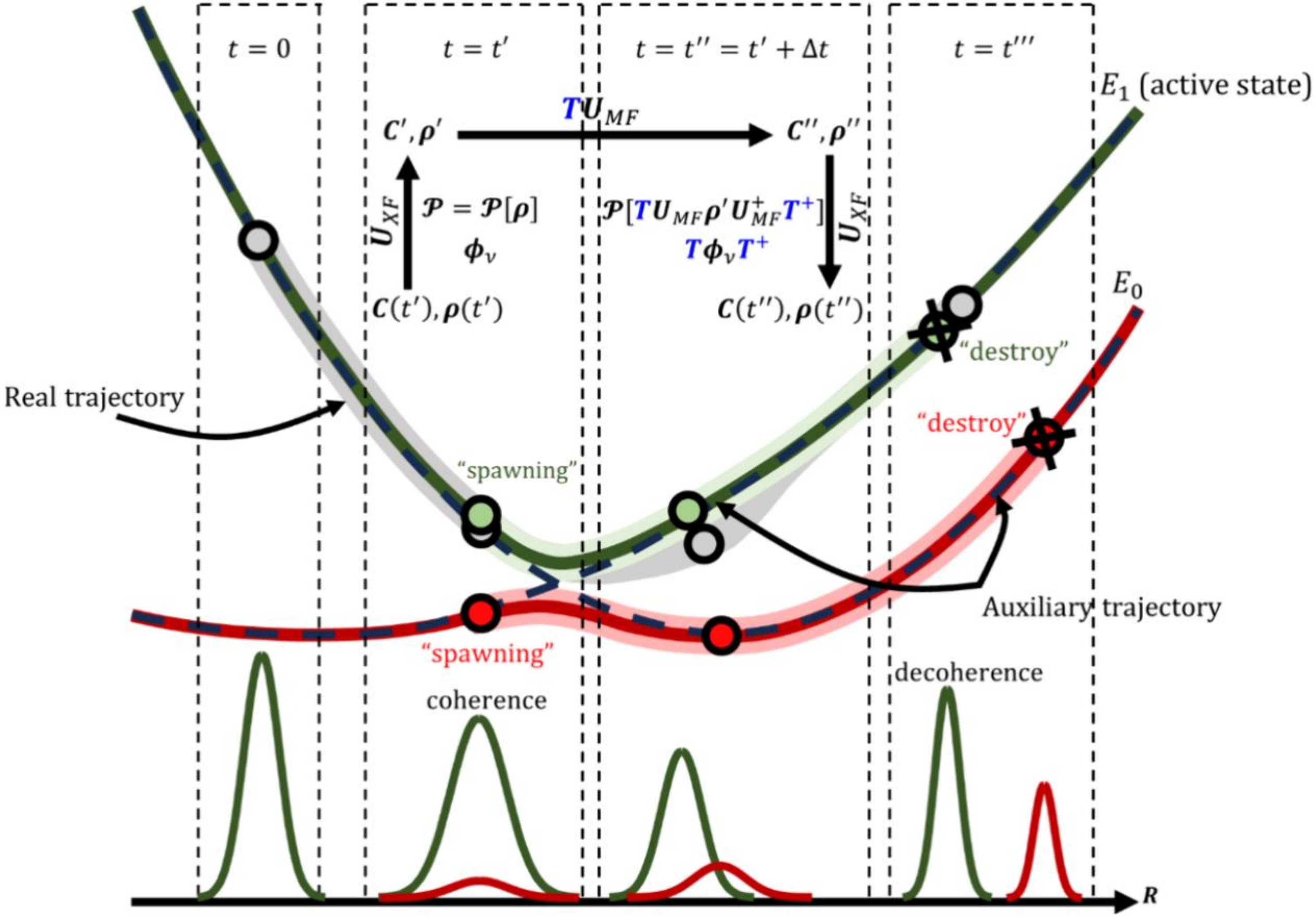

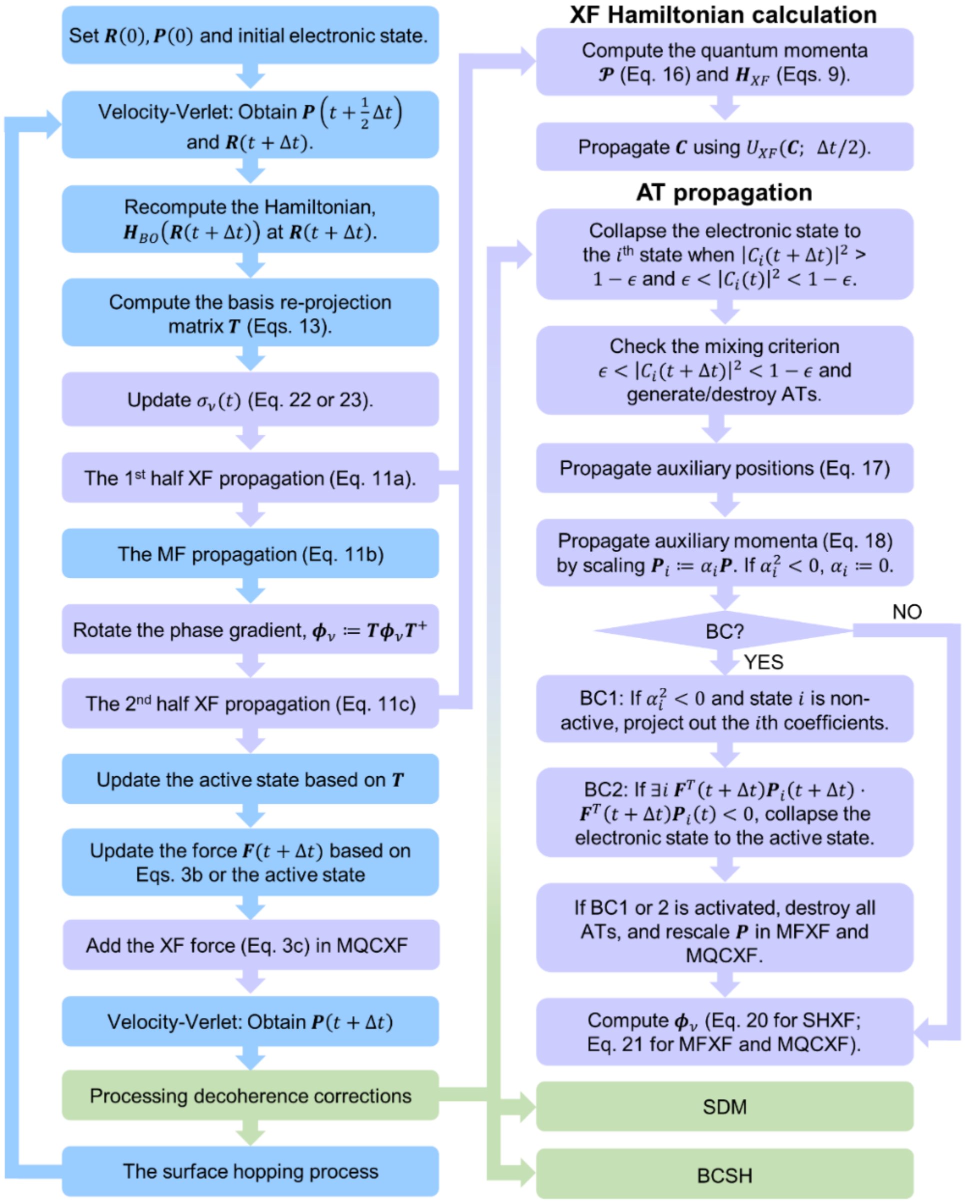

Han, D.; Akimov, A. V. *JCTC.* **2024**, *20* (12), 5022–5042.